



Truss optimization with multiple frequency constraints and automatic member grouping

José P. G. Carvalho¹ · Afonso C. C. Lemonge¹ · Érica C. R. Carvalho² ·
Patrícia H. Hallak¹ · Heder S. Bernardino³

Received: 26 December 2016 / Revised: 15 May 2017 / Accepted: 4 July 2017 / Published online: 29 July 2017
© Springer-Verlag GmbH Germany 2017

Abstract This paper deals with sizing and shape structural optimization problems with respect to the minimization of the masses of truss structures considering multiple natural frequencies as the constraints of the problems. The sizing and shape design variables are discrete and continuous, respectively. It can be attractive to use a reduced number of distinct cross-sectional areas minimizing costs of fabrication, transportation, storing, checking, welding, and so on. Also, it is expected a labor-saving when the structure is welded, checked and so on. On the other hand, one can observe that the task of discovering the optimum member grouping is not trivial and leads to an exhaustive trial-and-error process. Cardinality constraints are adopted in

order to obtain an automatic variable linking searching for the best member grouping of the bars of the trusses analyzed in this paper. A CRPSO (Craziness based Particle Swarm Optimization) is the search algorithm adopted in this paper. This algorithm uses a modified velocity expression and an operator called “craziness velocity” in order to avoid premature convergence. An Adaptive Penalty Method is adopted to handle the constraints. Six truss structures are analyzed, presenting very interesting results providing curves of tradeoff between the optimized weights versus the number of distinct cross-sectional areas used in these solutions.

Keywords Cardinality constraints · Multiple frequency constraints · Automatic member grouping

✉ Afonso C. C. Lemonge
afonso.lemonge@ufjf.edu.br

José P. G. Carvalho
jose.carvalho@engenharia.ufjf.br

Érica C. R. Carvalho
ericacarvalho@gmail.com

Patrícia H. Hallak
patricia.hallak@ufjf.edu.br

Heder S. Bernardino
heder@ice.ufjf.br

¹ Department of Applied and Computational Mechanics,
Faculty of Engineering, Federal University of Juiz de Fora,
Juiz de Fora, Brazil

² Postgraduate Program in Computational Modeling,
Federal University of Juiz de Fora, Juiz de Fora, Brazil

³ Department of Computer Science, Institute of Exact Sciences,
Federal University of Juiz de Fora, Juiz de Fora, Brazil

1 Introduction

Recent advances in structural engineering and the development of computational resources have allowed the implementation of more realistic models. For instance, the structural analysis due to dynamic actions, which were often times neglected in the past, are very important.

In the field of structural optimization, when the designer is faced with structural problems that require analysis involving dynamic actions, it must be included in the formulation of the problems. For example, the introduction of multiple natural frequencies as constraints leads to a highly nonlinear problem that has been investigated (Bellagamba and Yang 1981; Kaveh and Zolghadr 2012). This paper aims to address structural optimization problems of plane and space trusses subject to multiple natural frequencies of vibration as constraints. The problems analyzed here refer

to the weight minimization of truss structures where the cross-sectional areas of the bars and the node coordinates are the design variables, i.e., sizing and sizing/shape optimization.

Evolutionary Algorithms (EAs) are inspired by the natural processes of the real world. Some of them, like Particle Swarm Optimization (PSO) (Eberhart and Kennedy 1995), provide computational models based on the concept of collective intelligence. In this paper, a modified PSO called CRPSO (Craziness based Particle Swarm Optimization) and proposed by Kar et al. (2012) is used as a search algorithm. The CRPSO uses a modified velocity expression associated with a set of random numbers and an operator, with a pre-defined probability, called “craziness velocity”. It is not an objective of this paper to conduct a sensitivity analysis of the CRPSO such as all the parameters usually indicated to be set for the best performance of the algorithm.

Also, the CRPSO is adapted in this paper with a special encoding of the candidate particles for handling with cardinality constraints (Barbosa and Lemonge 2005), limiting the maximum number of distinct cross-sectional areas to be used in an optimized solution. This type of constraint is important because it can lead to economies of bulk purchasing, checking, welding, and freeing the designer of the task of deciding how to group members and/or design variables. A new test-bed for the literature is provided in this paper by using cardinality constraints to discover new member groupings. Here, the constrained problems are transformed into an unconstrained problems by introducing an Adaptive Penalty Method (APM) proposed by Barbosa and Lemonge (2002).

The remainder of the paper is organized as follows. Section 2 presents a brief review the structural optimization problems similar to those discussed in this paper. Section 3 describes the optimization problem discussed in this paper. Section 3.1 summarizes the automatic member grouping by using cardinality constraints. Section 4 describes the CRPSO algorithm and the penalty scheme. The computational experiments are presented in three section: i) Section 6 presents the analyses of the traditional problems from the literature providing a comparison with several references as well as the standard PSO and the adopted CRPSO used in this paper; ii) Section 6.1 presents the main purpose of this paper considering a special encoding for the automatic sizing design variable linking applying cardinality constraints, searching for the best member groupings of the test-problems discussed in the previous section; Finally, Section 7 presents the analyses of large-scale problems showing the performance of the proposed strategy to solve this type of complex optimization problems. The paper ends with conclusions and future work in Section 8.

2 Related work

This section attempts to summarize the recent literature on EAs to solve structural optimization problems with multiple natural frequencies as constraints as well as proposed methods or strategies to find optimal member groupings of bars.

A recently and important paper was published by Stolpe (2016) where is presented a critical review on truss optimization with discrete design variables. The author presented a survey with a reasonable set of references. Among them, several discussing optimization problems considering multiple natural frequencies as constraints. Some of them are described following.

Gomes (2011) investigated the use of a particle swarm optimization (PSO) as an optimization engine for structural truss mass optimization considering size and shape design variables and with frequency constraints. Four examples widely reported in the literature (10-, 37-, 52- and 72-bar trusses) were analyzed and the results show that the algorithm performed similarly to the other methods and even better in some cases.

Two of the most recent metaheuristics developed in the last decade, Harmony Search (HS) and Firefly Algorithm (FA), are proposed by Miguel and Miguel (2012) to solve truss shape and sizing optimization with multiple natural frequency constraints. The results showed that both metaheuristics reached, in a relatively low computational time, better results than reported in the literature.

Kaveh and Zolghadr (2014) presented a new algorithm called Democratic Particle Swarm Optimization for structural optimization with frequency constraints. Four numerical examples (10-, 37-bar trusses and 52-, 200-bar dome) were solved, indicating the viability of the proposed algorithm.

Size and shape optimization of truss structures was performed by Kaveh and Javadi (2014) using an efficient hybrid method: Harmony Search (HS) and Ray Optimizer (RO). Multiple frequency constraints were considered making the optimization a highly nonlinear problem. Some basic benchmark problems were solved by that hybrid method, and the numerical results indicate the efficiency and robustness of that method when compared to other heuristics in the literature.

Three modified versions of the SOS (Symbiotic Organism Search), algorithm are proposed by Tejani et al. (2016a). They are tested for suitability in applications to engineering structures subjected to dynamic excitation, which may lead to undesirable vibrations. To check the viability and efficiency of the proposed algorithms, six different planar and space trusses are subjected to experimental analysis. The results obtained using the proposed methods are

compared to those obtained using other optimization methods well established in the literature.

A modified sub-population teaching-learning-based optimization (MS-TLBO) algorithm is proposed by Tejani et al. (2016b) to improve exploration and exploitation capacities. The viability and efficiency of the proposed method are tested in five structural benchmark problems involving shape and size optimization with multiple natural frequency constraints on the planar and space trusses. The results reveal that MS-TLBO is more effective when compared to the original TLBO and other state-of-the-art algorithms.

Farshchin et al. (2016) introduce a multi-class teaching-learning-based optimization (MC-TLBO) technique for structural optimization with frequency constraints. The MC-TLBO algorithm is applied to some benchmark truss optimization problems (10-, 37-, 72-, 200-bar trusses and 52-bar truss dome) with frequency constraints to examine the efficiency of the proposed methodology. The obtained designs are compared to the results of both a modified TLBO algorithm and other optimization methods.

The automatic member grouping in structural optimization is clearly desirable but there are few papers in the literature presenting methods to solve this issue. Advantages in fabrication, checking, assembling, transportation and welding, which are usually not explicitly included in the cost function, are thus expected. Previous work can be found in Biedermann and Grierson (1995), which presented a GA coupled to a computer program called SODA (Structural Optimization Design & Analysis) to automate the design of building structures (Grierson and Cameron 1987). By using neural networks, Biedermann & Grierson proposed the representation of heuristic design knowledge in order to discover desirable member groupings of steel frame structures (Biedermann 1997; Biedermann and Grierson 1996). A multiobjective genetic algorithm was proposed by Galante (1996) and Shea et al. (1997) proposed a shape annealing approach to optimal truss design with dynamic grouping of members.

Barbosa and Lemonge (2005) proposed a genetic algorithm encoding which is able to automatically satisfy a class of important cardinality constraints where the set of distinct values of the design variables must be a subset – of cardinality not exceeding a given value – of a larger set of available items. Good results have been found in the minimization of truss structures and an extension of the proposed method was applied to other benchmark problems considering sizing and shape/sizing optimization presented in Barbosa et al. (2008).

Lemonge et al. (2010) proposed a GA to solve the configuration, shape, and sizing design for weight minimization of a dome structure and using cardinality constraints do discover desirable member groupings where the special

encoding in the GA presented continuous and discrete design variables. They again used a multiple cardinality constraint to search for optimized space-framed structures. In that paper, the columns and beams are linked in independent groups and an additional discrete design variable is considered corresponding to the orientation of the cross-section of the AISC profiles searched for the columns with respect to their principal axes. Further, inspired again by the special encoding proposed in Barbosa and Lemonge (2005) and Lemonge et al. (2011b) extended the previous work to the optimization of framed structures involving sizing design variables. They proposed in that paper a new encoding to handle multiple cardinality constraints in order to group beams and columns independently.

In 2010 Herencia and Haftka (2010) proposed a combined genetic algorithm-gradient strategy to find the minimum weight of the well known ten-bar truss for various numbers of cross-sectional areas. The idea is to restrict the maximum number of distinct cross-sections in the final weight of the truss. Inspired in the previous paper (Herencia et al. 2013) solved a structural optimization problem of composite structures, under strength and buckling constraints, limiting the maximum number of distinct cross-sectional areas in the final weight of the structure.

Liu et al. (2012) studied the optimum conceptual design of pile foundations at the initial design stage. A minimum-cost optimization model with multiple design constraints based on Chinese code and a cardinality constraint is built to achieve the concurrent optimization of pile size and layout. The model was solved by the improved automatic grouping genetic algorithms, proposed by Barbosa et al. (2008), to obtain the optimal grouping. A practical example indicates the efficiency of the proposed approach. Liu et al. (2012) also studied singular optimum topology of skeletal structures with frequency constraints. The topology optimization of frame structures has the characteristics of singular optimum and disjoint feasible domain. Because the discrete nature of such problems, the optimum design can not be obtained by continuous search. To deal with this difficulty, the automatic grouping genetic algorithm with improvements in crossover operator and penalty function are applied to optimize frame structures. Two examples (10-, 72- bar trusses) indicated the effectiveness of the proposed approach.

Kripka et al. (2013) demonstrated the application of optimization strategies for the cost of beams in reinforced concrete buildings. Since the number of beams of different sizes must be limited for practical reasons, cardinality constraints are also considered, aiming to identify the ideal grouping of elements. Some results obtained for different numbers of member groups are presented in order to illustrate the proposed procedure. Kripka et al. (2015) also performed an

automatic determination of the optimized group, taking into account the required maximum number of groups. Several numerical analyses were performed using the computational implementation of the developed formulation. These results provide evidence that the chosen procedure may provide a significant reduction in the cost of a structure, even for a small number of different cross-sections.

Two Ant Colony Optimization algorithms are proposed by Angelo et al. (2015) to tackle multi-objective structural optimization problems with cardinality constraint. Such constraint is directly enforced when an ant builds a candidate solution. The results obtained are compared with solutions available from single-objective studies in the literature.

Optimal design of dome structures with dynamic frequency constraints was discussed by Kaveh and Ghazaan (2016) using a strategy based on cascading that reduces the objective function value over a number of optimization stages by initially considering a small number of design variables which is gradually increased in the next stages.

It is important to cite relevant researches in this area from the literature as the papers of Rajeev and Krishnamoorthy (1992), Rajan (1995), and Galante (1996). These papers consider simultaneously sizing, shape and topology optimization and also discrete search spaces.

Very important references in the literature, especially those using gradient based methods, have to be cited in this section such as the problem of optimum truss topology design based on the ground structure approach proposed by Achtziger (1996) where the case when different properties of the bars for tension and for compression additionally are taken into account. In Achtziger (1997) proposed a topology optimization of discrete structures providing a self-constrained introduction and stresses the technique of reformulating problems and mathematical tools needs for a good performance of numerical treatments in the discussed problems presented in this paper.

New terminologies and an exact problem formulation are provided by Achtziger (1999a). It turns out that the classical constraints with respect to equilibrium and stress together with topological local buckling constraints do not necessarily guarantee the existence of a solution structure. Further, the same author in Achtziger (1999b) discussed a numerical approach to nonconvex and largescale problem.

In Achtziger and Kočvara (2007a) used a classic formulation of the topology optimization problem of discrete where the objective function to be maximized is the smallest natural frequency of the structure. They non-heuristic mathematical models with special attention to the situation when some design variables take zero values.

Achtziger and Kočvara (2007b) consider different problem formulations of topology optimization of discrete

structures with eigenvalues as constraints or as objective functions. They study multiple-load case formulations of minimum volume or weight, minimum compliance problems, and the problem of maximizing the minimal eigenvalue of the structure, including the effect of nonstructural mass.

A natural generator of optimum topology of plane trusses for specified fundamental frequency was proposed by Nakamura and Ohsaki (1992).

Recently, book published by Ohsaki (2016) covers since various formulations of structural optimization, topology and configuration of trusses to optimization of spatial trusses and building frames. This book also treats structural optimization problems with natural frequencies as constraints.

Chun et al. (2012) introduce a new method for incorporating random vibration theories into topology optimization in order to satisfy probabilistic constraints. This proposed method uses a discrete representation method for stochastic processes to describe the stochastic response of a system subjected to random seismic excitations. A new formulation is developed for sensitivity of dynamic responses in order to use gradient-based optimization algorithms for the proposed topology optimization employing a discrete representation method.

Rubio et al. (2011) studies the design of piezoelectric devices aimed at dynamic-type applications tailoring specified vibration modes as a requirement for designing. A technique for designing the shape of specified vibration modes is the topology optimization method (TOM) which finds an optimum material distribution inside a design domain to obtain a structure that vibrates according to specified eigenfrequencies and eigenmodes.

A versatile polygonal elements along with a multiresolution scheme for topology optimization to achieve computationally efficient and high resolution designs for eigenfrequency structural optimization problems is proposed by Filipov et al. (2016).

3 The structural optimization problem

The problems analyzed in this paper refer to sizing and sizing/shape optimization. The design variables are the cross-sectional areas (discrete) of the bars and the node coordinates (continuous). The optimization problem can be written as: find a set of cross-sectional areas $\mathbf{a} = \{A_1, A_2, \dots, A_N\}$ and the coordinates of a given nodes of the structure X_i, Y_i, Z_i , that minimizes its weight W .

$$W(\mathbf{a}) = \sum_{i=1}^N \rho A_i L_i \quad (1)$$

subject to frequency constraints

$$1 - \frac{f_j}{\bar{f}} \leq 0, \quad 1 \leq j \leq n_c \quad (2)$$

where ρ is the density of material, A_i is the cross-sectional area and L_i is the length of the i -th bar. The j -th natural frequency of the structure is denoted by f_j and \bar{f} is the lower (or upper) limit for the j -th allowed natural frequency of the structure. The number of bars of the structure is denoted by N and n_c is the number of constraints of the problem. It is important to note that the values of L_i can be changed when the shape is modified.

The natural frequencies are obtained by the evaluation of the eigenvalues of the matrix $[(f_{n_f}^2 * M) + K]$ (Bathe 2006), where M and K are the mass and stiffness matrices, respectively, and f_{n_f} are the equivalent eigenvectors with respect to the n_f natural frequencies of the structure.

3.1 Automatic member grouping and cardinality constraints

In order to explore desirable advantages during the design configurations it can be interesting to explore architec-tonic effects linking the members in groups. For instance, a designer may require that at most a given m of distinct cross-sectional areas should be used in the whole structure, leading to the need of arranging all bars in only m groups.

Thus, the optimization problem must consider additional constraints requiring that no more than m ($m \leq N$) different cross-sectional areas should be used, that is,

$$A_i \in C_m = \{S_1, S_2, \dots, S_m\}, \quad i = 1, 2, \dots, N$$

where the cross-sectional areas $S_j, j = 1, 2, \dots, m$ are unknown but belong to a larger ($M > m$) given set $S = \{A_1, A_2, \dots, A_M\}$. These additional constraints are defined as cardinality constraints and the standard structural optimization problem (without the cardinality constraint) is recovered when $m = N$.

An example of encoding of a particle with 12 design variables is presented in Fig. 1. This encoding is inspired by the chromosome proposed by Barbosa and Lemonge (2005). The cardinality constraints, for instance $m = 2$, are represented by the two variables at the left part of the encoding. At the right part of the encoding there are, in this illustration, 10 indexes that point to the design variables of the left part. These indexes point to a table with a given number of discrete values (cross-sectional areas of bars) able to be chosen. In this example, design variable 1 points to index 2, returning the value 2.7165 cm^2 , and design variable 2 points to index 19, returning 37.9286 cm^2 . At the right part of the encoding, for example, the fourth design variable points to the first design variable of the left part and the bar referred by this design variable has the cross-sectional area of 2.7165 cm^2 .

4 The CRPSO algorithm and the penalty scheme

Particle Swarm Optimization (PSO) was originally introduced by Kennedy & Eberhart (Eberhart and Kennedy 1995). The algorithm was inspired by the social behavior of birds flocking. PSO is a population-based algorithm with fewer parameters to be set and is easier to implement than other EA's. The objective function is evaluated for each

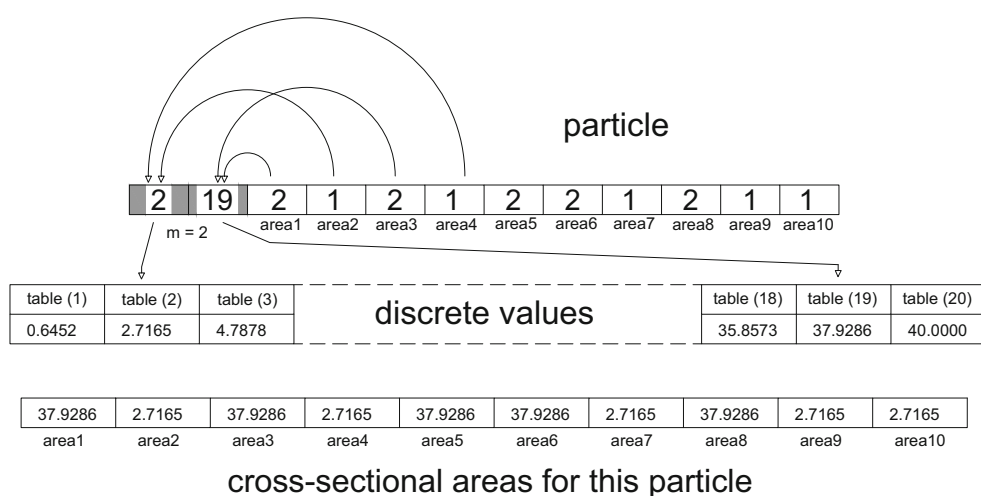


Fig. 1 Example of the encoding of a particle with 12 design variables. The cardinality constraints ($m = 2$) are represented by the two variables at the left part of the vector which represents the particle. At the

right part of the vector there are, for instance, 10 indexes that point to the the design variables at the left part

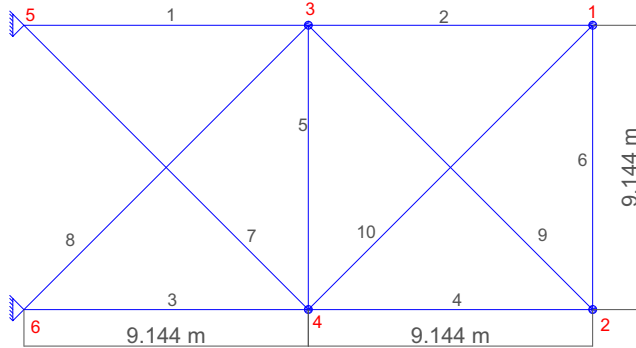


Fig. 2 10-bar truss

particle and the fitness value of particles is obtained in order to determine which position in the search space is the best.

In each iteration t of the CRPSO, the swarm is updated using the following equations:

$$\begin{aligned} v_j^{(i)}(t+1) &= v_j^{(i)}(t) + c_1 \cdot r_1(x_{pbest}^{(i)}(t) - x_j^{(i)}(t)) \\ &\quad + c_2 \cdot r_2(x_{gbest}(t) - x_j^{(i)}(t)) \end{aligned} \quad (3)$$

$$x_j^{(i)}(t+1) = x_j^{(i)}(t) + v_j^{(i)}(t+1) \quad (4)$$

where $v_j^{(i)}$ and $x_j^{(i)}$ represent the current velocity and the current position of the j th design variable of the i th particle, respectively. $x_{pbest}^{(i)}$ is the best previous position of the i th particle (called $pbest$) and x_{gbest} is the best global position among all the particle in the swarm (called $gbest$); c_1 and c_2 are coefficients that control the influence of cognitive and social information, respectively, and r_1 and r_2 are two uniform random sequences generated between 0 and 1.

A change in the conventional PSO algorithm, called Craziness-based Particle Swarm Optimization (CRPSO) and proposed by Kar et al. (2012), is used here in order to improve the PSO behavior, thus avoiding premature convergence. A new velocity expression v_i , associated with a set of random numbers and an operator called “craziness velocity”, is considered. The operator has a predefined

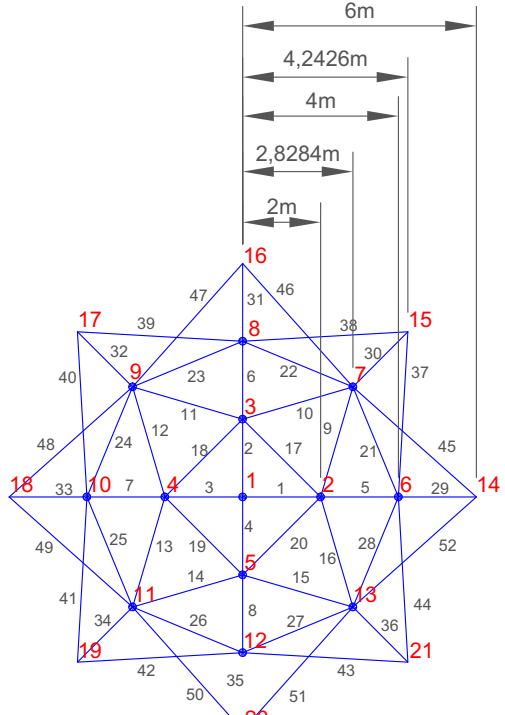


Fig. 4 52-bar truss dome – top view

probability of craziness. In this case the velocity can be expressed as follows (Kar et al. 2012):

$$\begin{aligned} v_j^{(i)}(t+1) &= r_2 \cdot sign(r_3) \cdot v_j^{(i)}(t) + (1-r_2)c_1 \\ &\quad \cdot r_1 \left(x_{pbest}^{(i)} - x_j^{(i)} \right) + (1-r_2) \cdot c_2 \cdot \\ &\quad (1-r_1) \left(x_{gbest} - x_j^{(i)} \right) + P(r_4) \\ &\quad \cdot sign2(r_4) \cdot v_j^{craziness} \end{aligned} \quad (5)$$

where r_1, r_2, r_3 and r_4 are the random parameters uniformly taken from the interval $[0,1]$, $sign(r_3)$ is a function defined as

$$sign(r_3) = \begin{cases} -1, & r_3 \leq 0.5 \\ 1, & r_3 > 0.5 \end{cases} \quad (6)$$

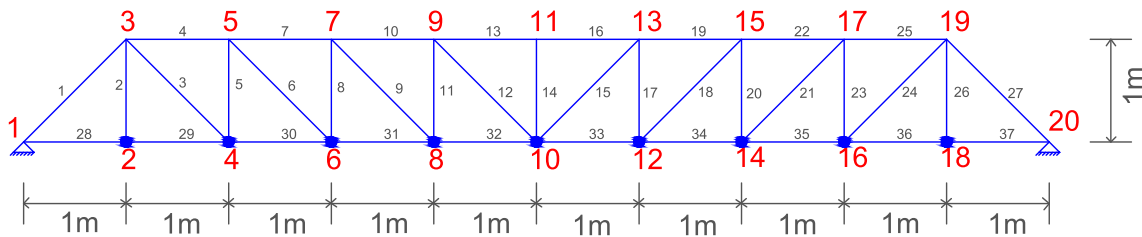


Fig. 3 A possible configuration for the 37-bar truss

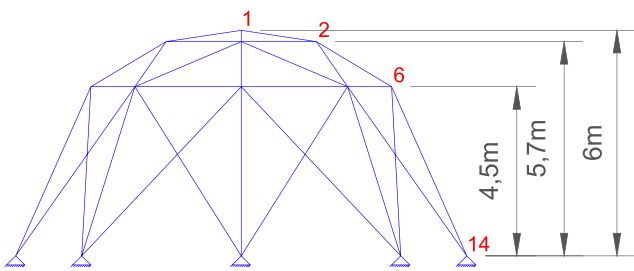


Fig. 5 52-bar truss dome – side view

$v_j^{craziness}$, the craziness velocity, is a user defined parameter from the interval $[v^{min}, v^{max}]$ and $P(r_4)$ and $sign2(r_4)$ are defined, respectively, as

$$P(r_4) = \begin{cases} 1, & r_4 \leq Pcr \\ 0, & r_4 > Pcr \end{cases} \quad (7)$$

$$sign2(r_4) = \begin{cases} -1, & r_4 \geq 0.5 \\ 1, & r_4 < 0.5 \end{cases} \quad (8)$$

and Pcr is a predefined probability of craziness. Although the parameter Pcr is fixed, $P(r_4)$ is defined every time the velocity is calculated.

To handle the constraints, a variant of the Adaptive Penalty Method introduced by Carvalho et al. (2015), is adopted here to enforce all the mechanical constraints considered in the numerical experiments. The fitness function $F(x)$ is defined as:

$$F(x) = \begin{cases} f(x), & \text{if } x \text{ is feasible} \\ \bar{f}(x) + \sum_{j=1}^{n_c} k_j v_j(x), & \text{otherwise} \end{cases} \quad (9)$$

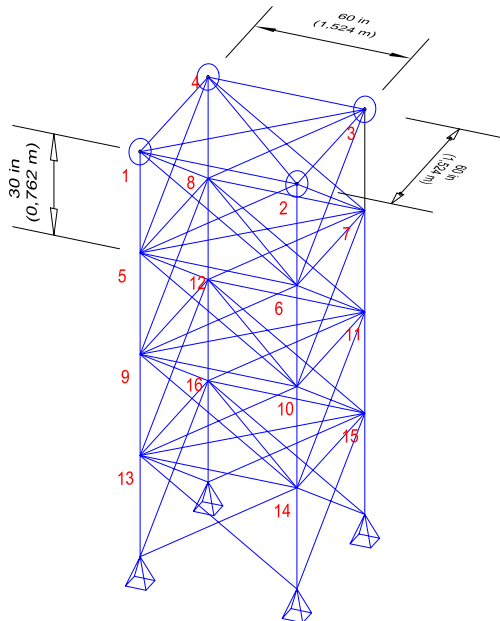


Fig. 6 72-bar truss

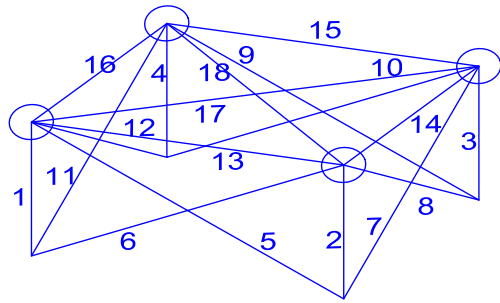


Fig. 7 72-bar truss - pattern module

and

$$\bar{f}(x) = \begin{cases} f(x), & \text{if } f(x) > \langle f(x) \rangle \\ \langle f(x) \rangle, & \text{if } f(x) \leq \langle f(x) \rangle \end{cases} \quad (10)$$

where $\langle f(x) \rangle$ is the average value of the objective function of the current population. The penalty parameter k_j is defined as

$$k_j = |\langle f(x) \rangle| \frac{\langle v_j(x) \rangle}{\sum_{l=1}^{n_c} [\langle v_l(x) \rangle]^2} \quad (11)$$

where $\langle v_j(x) \rangle$ means the violation of the j -th constraint averaged over the current population considering only infeasible individuals.

5 Computational experiments

The computational experiments refer to the structural optimization of six truss structures where two of them are planar structures (10- and 37-bar trusses), and the others are space structures (52-bar truss dome, 72-bar truss, 600-bar single layer and 1410-bar double layer truss domes). The experiments analyzed in this paper are similar to those presented in Kaveh et al. (2015a), Kaveh and Javadi (2014), Kaveh and Zolghadr (2014), and Kaveh and Ghazaan (2016).

The discrete design variables are considered here as the nearest integer of the corresponding variable of the vector solution (particle), as used in Vargas et al. (2015).

The PSO used continuous design variables and $c_1 = c_2 = 2.05$. The CRPSO used continuous design variables, $v_j^{craziness} = 0.001$, $c_1 = c_2 = 2.05$ and $Pcr = 0.5$.

The numerical experiments are divided in three sets.

- The first one discuss the benchmark test-problems with the same formulations presented in Kaveh et al. (2015a) and Kaveh and Javadi (2014) for the 10-, 37-, 52- and 72-bar trusses. The performance of the standard PSO and the adopted CRPSO are compared in this section.
- The second one refers to the use the CRPSO to solve the optimization problems considering cardinality constraints to find the best member groupings for the

Table 1 Optimum results for 10-bar truss. Cross-sectional areas in (cm²)

dv	References							
	(Kaveh and Farhoudi 2013)	(Sedaghati 2005)	(Kaveh and Farhoudi 2011)	(Kaveh and Javadi 2014)	(Kaveh and Zolghadr 2014)	(Kaveh et al. 2015b)	PSO	CRPSO
A ₁	36.584	38.245	32.456	35.944	35.540	35.300	47.400	35.400
A ₂	24.658	9.916	16.577	15.530	15.293	15.100	10.399	14.500
A ₃	36.584	38.619	32.456	35.285	35.784	36.500	36.899	35.500
A ₄	24.658	18.232	16.577	15.385	14.605	15.400	19.799	14.400
A ₅	4.167	4.419	2.115	0.648	0.645	0.645	4.299	0.645
A ₆	2.070	4.194	4.467	4.583	4.625	4.600	5.100	4.700
A ₇	27.032	20.097	22.810	23.610	24.778	23.700	18.300	24.500
A ₈	27.032	24.097	22.810	23.599	23.310	24.000	24.700	24.400
A ₉	10.346	13.890	17.490	13.357	12.482	11.500	11.800	12.800
A ₁₀	10.346	11.451	17.490	12.357	12.674	13.500	18.600	12.300
Natural frequencies								
f ₁ (Hz)	7.059	6.992	7.011	7.000	6.999	7.000	7.140	7.000
f ₂ (Hz)	15.895	17.599	17.302	16.187	16.175	16.208	17.769	16.161
f ₃ (Hz)	20.425	19.973	20.001	20.000	19.999	20.005	20.176	20.004
W (kg)	594.000	537.010	553.800	532.390	532.110	532.814	577.541	532.124
nfe	—	—	—	21000	—	21000	21000	21000

Table 2 Optimum results for 37-bar truss. Cross-sectional areas in (cm²) and node coordinates in meters – First analysis

dv	References								
	(Wang et al. 2004)	(Lingyun et al. 2005)	(Gomes 2011)	(Kaveh and Javadi 2014)	(Kaveh and Zolghadr 2011)	(Kaveh and Zolghadr 2014)	(Kaveh et al. 2015b)		
A ₁ , A ₂₇	3.250	2.893	2.679	2.851	2.908	2.620	2.7	3.8	3.0
A ₂ , A ₂₆	1.236	1.120	1.156	1.000	1.021	1.039	1.0	1.0	1.0
A ₃ , A ₂₄	1.000	1.000	2.347	1.834	1.036	1.046	1.0	1.0	1.0
A ₄ , A ₂₅	2.538	1.865	1.718	1.887	3.914	2.716	2.4	2.7	2.6
A ₅ , A ₂₃	1.371	1.596	1.275	1.062	1.002	1.025	1.2	1.0	1.0
A ₆ , A ₂₁	1.368	1.264	1.481	1.802	1.216	1.508	1.2	1.0	1.2
A ₇ , A ₂₂	2.429	1.825	4.685	1.933	2.714	2.375	2.2	3.7	2.6
A ₈ , A ₂₀	1.652	2.009	1.124	1.249	1.266	1.449	1.3	1.5	1.2
A ₉ , A ₁₈	1.825	1.952	2.121	1.874	1.8006	1.449	1.9	1.9	1.6
A ₁₀ , A ₁₉	2.302	1.970	3.860	1.957	4.027	2.532	2.2	1.9	2.5
A ₁₁ , A ₁₇	1.310	1.829	2.981	1.244	1.336	1.235	1.3	1.6	1.0
A ₁₂ , A ₁₅	1.406	1.235	1.202	1.777	1.054	1.352	1.4	1.0	1.3
A ₁₃ , A ₁₆	2.189	1.404	1.256	1.806	2.811	2.914	2.5	2.0	2.7
A ₁₄	1.000	1.000	3.327	1.000	1.170	1.008	1.0	1.0	1.0
Y ₃ , Y ₁₉	1.208	1.199	0.963	1.0744	0.872	0.948	1.04	1.281	0.877
Y ₅ , Y ₁₇	1.578	1.655	1.397	1.495	1.212	1.343	1.40	1.862	1.267
Y ₇ , Y ₁₅	1.671	1.965	1.592	1.732	1.382	1.504	1.64	2.000	1.455
Y ₉ , Y ₁₃	1.770	2.073	1.881	1.894	1.470	1.635	1.74	2.000	1.583
Y ₁₁	1.850	2.305	2.085	1.969	1.568	1.718	1.84	2.000	1.662
Natural frequencies									
f ₁ (Hz)	20.085	20.001	20.000	20.000	20.000	20.019	20.033	21.297	20.004
f ₂ (Hz)	42.074	40.030	40.000	40.016	40.069	40.011	40.346	40.699	40.000
f ₃ (Hz)	62.938	60.000	60.000	60.010	60.698	60.000	60.064	61.259	60.043
W (kg)	366.50	368.84	377.20	364.72	362.84	360.40	361.03	370.502	358.007
nfe	—	8000	—	24000	—	—	24000	24000	24000

Table 3 Optimum results for 52-bar truss dome. Cross-sectional areas in cm² and node coordinates in meters

<i>dv</i>	References								
	(Lin et al. 1982)	(Lingyun et al. 2005)	(Gomes 2011)	(Kaveh and Zolghadr 2012)	(Kaveh and Javadi 2014)	(Kaveh and Zolghadr 2014)	(Kaveh et al. 2015b)	PSO	CRPSO
<i>A</i> ₁ - <i>A</i> ₄	1.000	1.000	0.369	1.000	1.000	1.000	1.1	1.0	1.0
<i>A</i> ₅ - <i>A</i> ₈	1.330	2.141	4.191	1.305	1.136	1.139	1.2	1.0	1.2
<i>A</i> ₉ - <i>A</i> ₁₆	1.580	1.485	1.512	1.423	1.221	1.226	1.2	1.8	1.2
<i>A</i> ₁₇ - <i>A</i> ₂₀	1.000	1.401	1.562	1.385	1.486	1.333	1.6	1.0	1.5
<i>A</i> ₂₁ - <i>A</i> ₂₈	1.710	1.911	1.915	1.422	1.395	1.416	1.4	1.0	1.4
<i>A</i> ₂₉ - <i>A</i> ₃₆	1.540	1.010	1.131	1.000	1.000	1.000	1.0	1.0	1.0
<i>A</i> ₃₇ - <i>A</i> ₄₄	2.650	1.469	1.823	1.556	1.551	1.575	1.5	2.4	1.7
<i>A</i> ₄₅ - <i>A</i> ₅₂	2.870	2.141	1.090	1.448	1.418	1.435	1.5	1.7	1.3
<i>Z</i> ₁	4.320	5.885	5.534	5.331	5.828	6.112	5.72	4.000	5.554
<i>X</i> ₂	1.315	1.762	2.088	2.132	2.243	2.234	2.14	2.267	2.210
<i>Z</i> ₂	4.174	4.409	3.928	3.719	3.720	3.832	3.78	3.700	3.700
<i>X</i> ₆	2.916	3.440	4.025	3.935	3.956	4.031	3.94	3.919	3.921
<i>Z</i> ₆	3.267	3.187	2.457	2.500	2.500	2.503	2.52	2.500	2.500
Natural frequencies									
<i>f</i> ₁ (Hz)	15.220	12.810	12.751	12.987	11.685	11.315	11.410	13.869	12.529
<i>f</i> ₂ (Hz)	29.280	28.650	28.649	28.648	28.648	28.648	28.649	28.818	28.648
<i>W</i> (kg)	298.000	236.046	228.381	197.309	193.351	195.351	195.852	222.899	193.131
<i>nfe</i>	—	8000	—	—	27000	—	24000	24000	24000

Table 4 Optimum results for 72-bar truss. Cross-sectional areas in cm²

<i>dv</i>	References								
	(Konzelman 1986)	(Sedaghati 2005)	(Gomes 2011)	(Kaveh and Zolghadr 2012)	(Kaveh et al. 2015b)	PSO	CRPSO		
<i>A</i> ₁ - <i>A</i> ₄	3.499	3.499	2.987	3.949	3.60	8.800	3.700		
<i>A</i> ₅ - <i>A</i> ₁₂	7.932	7.932	7.749	7.968	8.100	8.000	8.000		
<i>A</i> ₁₃ - <i>A</i> ₁₆	0.645	0.645	0.645	0.645	0.645	0.645	0.645		
<i>A</i> ₁₇ - <i>A</i> ₁₈	0.645	0.645	0.645	0.647	0.645	0.645	0.645		
<i>A</i> ₁₉ - <i>A</i> ₂₂	8.056	8.056	8.765	7.525	8.85	24.000	8.000		
<i>A</i> ₂₃ - <i>A</i> ₃₀	8.011	8.011	8.153	7.863	8.50	7.800	7.900		
<i>A</i> ₃₁ - <i>A</i> ₃₄	0.645	0.645	0.645	0.645	0.70	0.645	0.645		
<i>A</i> ₃₅ - <i>A</i> ₃₆	0.645	0.645	0.645	0.652	0.645	0.645	0.645		
<i>A</i> ₃₇ - <i>A</i> ₄₀	12.812	12.812	13.450	12.966	11.850	14.000	13.100		
<i>A</i> ₄₁ - <i>A</i> ₄₈	8.061	8.061	8.073	8.347	8.10	6.200	7.900		
<i>A</i> ₄₉ - <i>A</i> ₅₂	0.645	0.645	0.645	0.645	0.645	2.600	0.645		
<i>A</i> ₅₃ - <i>A</i> ₅₄	0.645	0.645	0.645	0.645	0.645	0.645	0.645		
<i>A</i> ₅₅ - <i>A</i> ₅₈	17.279	17.279	16.684	17.389	17.60	15.900	16.800		
<i>A</i> ₅₉ - <i>A</i> ₆₆	8.088	8.088	8.159	8.006	7.55	12.600	8.300		
<i>A</i> ₆₇ - <i>A</i> ₇₀	0.645	0.645	0.645	0.645	0.645	0.645	0.645		
<i>A</i> ₇₁ - <i>A</i> ₇₂	0.645	0.645	0.645	0.645	0.645	0.645	0.645		
Natural frequencies									
<i>f</i> ₁ (Hz)	4.000	4.000	4.000	4.000	4.000	4.219	4.000		
<i>f</i> ₃ (Hz)	6.000	6.000	6.000	6.000	6.0080	6.034	6.004		
<i>W</i> (Kg)	327.605	327.605	328.823	328.589	329.422	391.864	328.215		
<i>nfe</i>	—	—	—	—	27000	27000	27000		

test-problems analyzed in the first set of the numerical experiments.

- The third one, presents the analyses of large-scale problems presented in Kaveh and Ghazaan (2016).

The following subsections present the description of the optimization problems discussed in the first and second set of numerical experiments. For these test-problems the number of particles is defined for each experiment: 70 for the 10-bar truss, 80 for the 37, 52 and 90 for the 72-bar truss and the number of function evaluations is displayed in the tables of results. The number of independent runs is 50 and the best solutions presented in the comparisons are rigorously feasible. The discrete search spaces are the same that were used in by Kaveh et al. (2015a). For the third set numerical experiments, 600-bar single layer dome truss and 1410 double layer dome truss, the population size are equal to 80 and 20 independent runs are performed.

5.1 10-bar truss

The first experiment is the 10-bar truss depicted in Fig. 2. The material has Young's modulus $E = 68.9$ GPa and density $\rho = 2770.00$ kg/m³. A nonstructural mass of 454.0 kg is added in each node. The sizing design variables are the cross-sectional areas of the bars. The values can be chosen from discrete set of (0.645, 0.7, 0.8, 0.9, ..., 50) cm². The limits for natural frequencies are $f_1 \geq 7$ Hz, $f_2 \geq 15$ Hz and $f_3 \geq 20$ Hz.

5.2 37-bar truss

This experiment corresponds to the weight minimization of a 37-bar truss with a possible shape configuration depicted in Fig. 3. A nonstructural mass of 10 kg is added at each node of the bottom chord. The material has Young's modulus $E = 210$ GPa and density $\rho = 7800$ kg/m³. The optimization problem considers sizing and shape design variables and symmetry must to be controlled by the axis between the line connecting nodes 10 and 11. The bars of the bottom chord (between nodes 1 and 20) have constant and pre-defined cross-sectional areas of 4×10^{-3} m². The nodes of the top chord have their coordinates as shape

Table 5 Statistical results for the first analysis of the numerical experiments

	Best	Median	Average	Std	Worst
10-bar truss	532.123	539.490	539.755	6.055	556.849
37-bar truss	358.007	359.504	361.347	5.066	381.234
52-bar truss	193.130	200.187	207.885	31.060	376.887
72-bar truss	328.214	328.364	332.722	29.469	378.978

Table 6 Results for the 10-bar truss, where areas A_i are in cm²

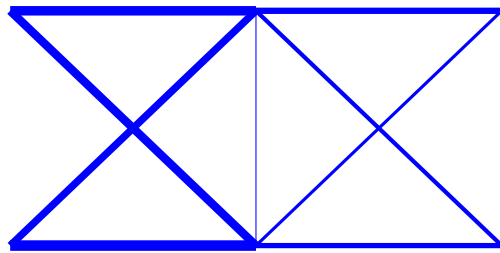
dv	$m = 1$	$m = 2$	$m = 3$	$m = 4$	no c.c. (10)
A_1	29.0	38.6	42.6	40.7	35.4
A_2	29.0	13.0	6.7	11.8	14.5
A_3	29.0	38.6	42.6	40.7	35.5
A_4	29.0	13.0	20.6	20.8	14.4
A_5	29.0	13.0	6.7	4.3	0.645
A_6	29.0	13.0	6.7	4.3	4.7
A_7	29.0	38.6	20.6	20.8	24.5
A_8	29.0	13.0	20.6	20.8	24.4
A_9	29.0	13.0	20.6	11.8	12.8
A_{10}	29.0	13.0	6.7	11.8	12.3
Natural frequencies					
f_1 (Hz)	7.008	7.002	7.000	7.000	7.000
f_2 (Hz)	21.061	18.842	16.311	18.279	16.162
f_3 (Hz)	22.615	20.026	20.116	20.002	20.005
W (kg)	858.041	606.489	565.448	545.226	532.124
nfe	21000	21000	21000	21000	21000

Table 7 Results for the 37-bar truss, where areas A_i are in cm² and the node coordinates Y_i are in meters

dv	$m = 1$	$m = 2$	$m = 3$	$m = 4$	no c.c. (8)
A_1, A_{27}	1.9	2.3	2.4	2.9	3.0
A_2, A_{26}	1.9	1.4	1.1	1.3	1.0
A_3, A_{24}	1.9	1.4	1.1	1.0	1.0
A_4, A_{25}	1.9	2.3	2.4	2.9	2.6
A_5, A_{23}	1.9	1.4	1.1	1.0	1.0
A_6, A_{21}	1.9	1.4	1.1	1.3	1.2
A_7, A_{22}	1.9	2.3	2.4	2.7	2.6
A_8, A_{20}	1.9	1.4	1.7	1.3	1.2
A_9, A_{18}	1.9	1.4	1.7	1.3	1.6
A_{10}, A_{19}	1.9	1.4	1.7	2.9	2.5
A_{11}, A_{17}	1.9	1.4	1.7	1.3	1.0
A_{12}, A_{15}	1.9	1.4	1.1	1.3	1.3
A_{13}, A_{16}	1.9	2.3	1.7	2.9	2.7
A_{14}	1.9	1.4	1.1	1.0	1.0
Y_3, Y_{19} (m)	1.026	1.032	1.021	0.800	0.877
Y_5, Y_{17} (m)	1.525	1.475	1.485	1.163	1.267
Y_7, Y_{15} (m)	1.840	1.714	1.734	1.382	1.455
Y_9, Y_{13} (m)	1.989	1.870	1.873	1.524	1.583
Y_{11} (cm)	2.000	1.958	2.000	1.585	1.662
Natural frequencies					
f_1 (Hz)	20.000	20.000	20.000	20.000	20.004
f_2 (Hz)	41.798	40.000	40.001	40.000	40.000
f_3 (Hz)	63.693	60.001	60.010	60.036	60.043
W (kg)	372.966	362.031	360.754	358.856	358.007
nfe	24000	24000	24000	24000	24000

Table 8 Results for the 52-bar truss, where areas A_i are in cm^2 and the node coordinates X_i and Z_i are in meters

dv	$m = 1$	$m = 2$	$m = 3$	$m = 4$	no c.c. (5)
A_1-A_4	1.5	1.0	1.0	1.0	1.0
A_5-A_8	1.5	1.5	1.4	1.2	1.2
A_9-A_{16}	1.5	1.5	1.4	1.4	1.2
$A_{17}-A_{20}$	1.5	1.5	1.5	1.2	1.5
$A_{21}-A_{28}$	1.5	1.5	1.4	1.4	1.4
$A_{29}-A_{36}$	1.5	1.0	1.0	1.0	1.0
$A_{37}-A_{44}$	1.5	1.5	1.4	1.6	1.7
$A_{45}-A_{52}$	1.5	1.5	1.5	1.4	1.3
Z_1 (m)	4.723	4.875	5.306	5.604	5.554
X_2 (m)	1.787	1.972	2.144	2.285	2.210
Z_2 (m)	3.701	3.701	3.701	3.701	3.700
X_6 (m)	3.800	3.850	3.909	3.955	3.921
Z_6 (m)	2.501	2.501	2.501	2.506	2.500
Natural frequencies					
f_1 (Hz)	15.915	15.915	13.702	13.411	12.529
f_2 (Hz)	28.648	28.648	28.648	28.648	28.648
W (kg)	211.605	199.501	194.276	194.886	193.131
nfe	24000	24000	24000	24000	24000

**Fig. 8** The best result for the 10-bar truss without cardinality constraints

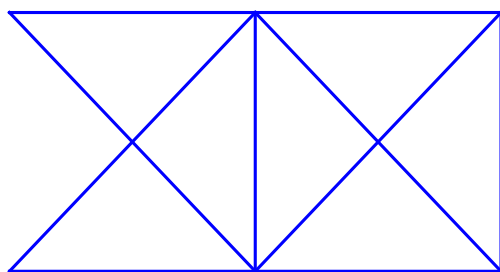
design variables in the vertical direction. The search space for the sizing design variables can be chosen from discrete set of $(1.0, 1.1, 1.2, 1.3, \dots, 10) \text{ cm}^2$. Thus, there is a total of 19 design variables where 5 are for the shape and 14 are for the sizing. The natural frequencies have the following limits to be satisfied: $f_1 \geq 20 \text{ Hz}$, $f_2 \geq 40 \text{ Hz}$ and $f_3 \geq 60 \text{ Hz}$.

5.3 52-bar truss dome

This experiment corresponds to the weight minimization of the 52-bar truss dome depicted in Figs. 4 and 5. The material has Young's modulus $E = 210 \text{ GPa}$ and density $\rho = 7800 \text{ kg/m}^3$ and a nonstructural mass of 50 kg is considered for every free node. In this experiment there is both sizing and shape optimization. In the shape optimization, node coordinates can move $\pm 2.0 \text{ m}$, and, in the sizing optimization, the areas are grouped into 8 groups. The symmetry in xy plane is kept and the nodes in the same elevation maintain the same z coordinates. There are 13 independent design variables, 8 for sizing and 5 for shape. The search space for the sizing design variables can be chosen from discrete set of $(1.0, 1.1, 1.2, 1.3, \dots, 10) \text{ cm}^2$. The frequency constraints are $f_1 \leq 15.9155 \text{ Hz}$ and $f_2 \geq 28.6479 \text{ Hz}$.

5.4 72-bar truss

The last experiment corresponds to weight minimization of the 72-bar truss depicted in Figs. 6 and 7 where the

**Fig. 9** The best result for the 10-bar truss with cardinality constraints for $m = 1$

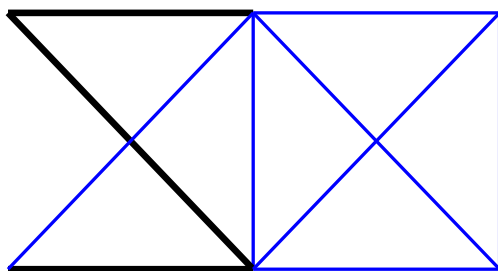


Fig. 10 The best result for the 10-bar truss with cardinality constraints for $m = 2$

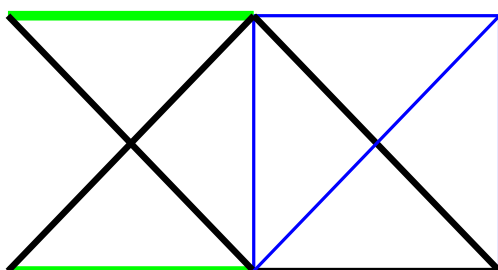


Fig. 11 The best result for the 10-bar truss with cardinality constraints for $m = 3$

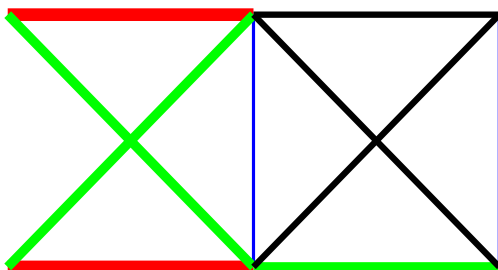


Fig. 12 The best result for the 10-bar truss with cardinality constraints for $m = 4$

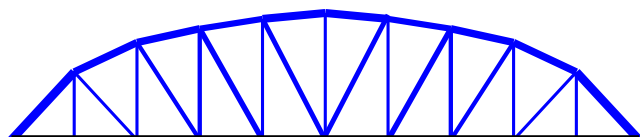


Fig. 13 The best result for the 37-bar truss without cardinality constraints

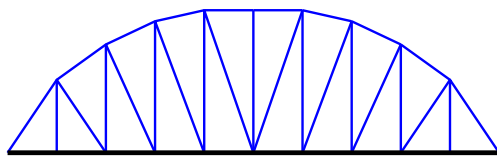


Fig. 14 The best result for the 37-bar truss with cardinality constraints for $m = 1$

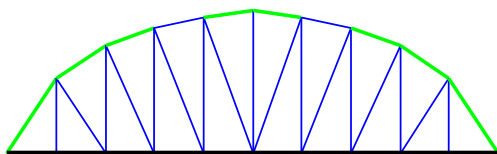


Fig. 15 The best result for the 37-bar truss with cardinality constraints for $m = 2$

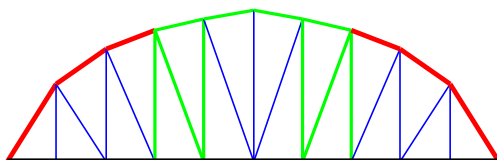


Fig. 16 The best result for the 37-bar truss with cardinality constraints for $m = 3$

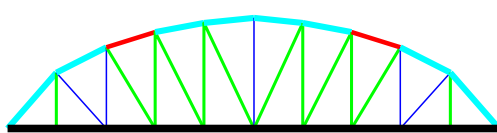


Fig. 17 The best result for the 37-bar truss with cardinality constraints for $m = 4$

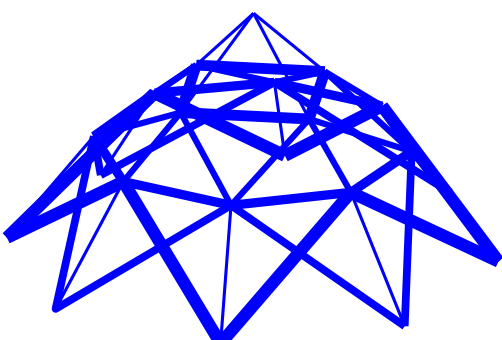


Fig. 18 The best result for the 52-bar truss dome without cardinality constraints - 3D view

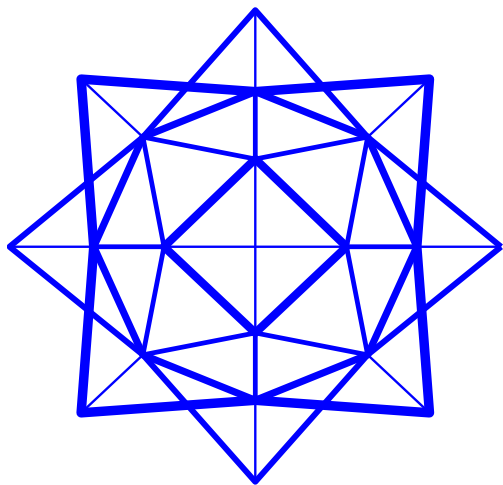


Fig. 19 The best result for the 52-bar truss dome without cardinality constraints - top view

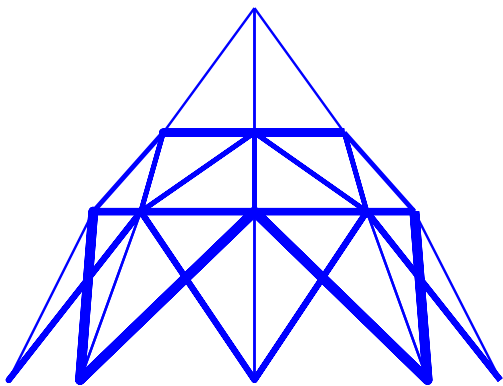


Fig. 20 The best result for the 52-bar truss dome without cardinality constraints - side view

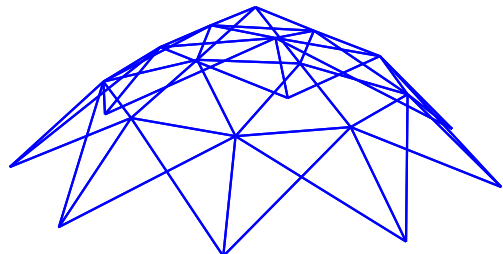


Fig. 21 The best result for the 52-bar truss dome with cardinality constraints for $m = 1$

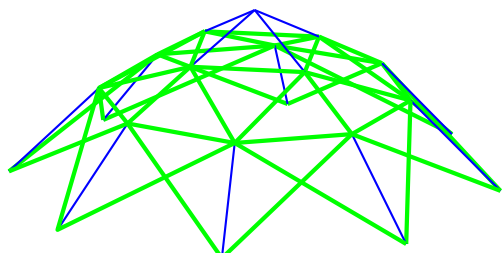


Fig. 22 The best result for the 52-bar truss dome with cardinality constraints for $m = 2$

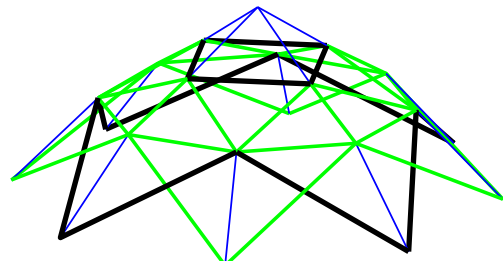


Fig. 23 The best result for the 52-bar truss dome with cardinality constraints for $m = 3$

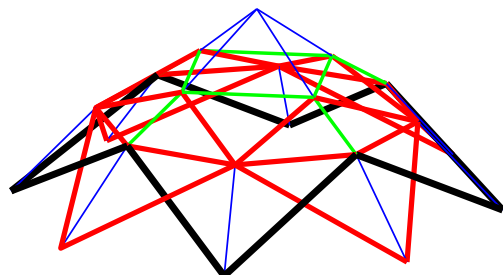


Fig. 24 The best result for the 52-bar truss dome with cardinality constraints for $m = 4$

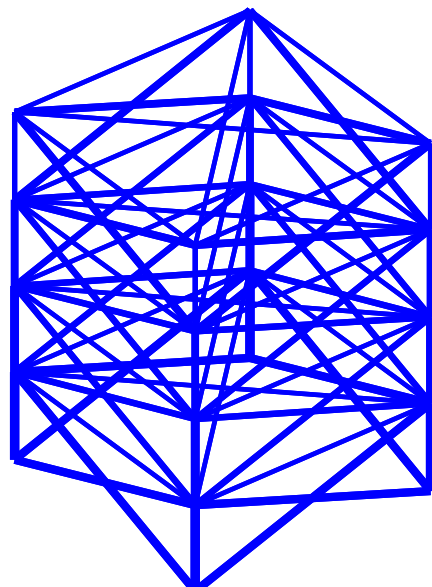


Fig. 25 The best result for the 72-bar truss without cardinality constraints

bars are linked as indicated in Table 9. A nonstructural mass of 2270.00 kg (5000 lbs) is added at the four nodes at the top of the truss. The material has Young's modulus $E = 68.9$ GPa and density $\rho = 2770.00$ kg/m³. The discrete search for the sizing design variables can be chosen from discrete set of (0.645, 0.7, 0.8, 0.9, ..., 50) cm². The natural frequencies have the limits $f_1 \geq 4$ Hz and $f_3 \geq 6$ Hz.

6 The first set of numerical experiments

In order to assess the performance of the CRPSO, the experiments were performed firstly using the standard PSO and CRPSO. All of results obtained by these two algorithms are compared with those presented by Kaveh et al. (2015b).

The CRPSO used in this paper presented a better performance when compared with the standard PSO, observing the results presented in Tables 1, 2, 3 and 4, where dv means design variable and W the final weight. For the 10-bar truss, 532.124 kg against 577.541 kg; for the 37-bar truss, 358.007 kg against 370.502 kg; for the 52-bar truss dome, 193.131 kg against 222.899 kg; and finally, for the 72-bar truss, 328.215 kg against 391.864 kg.

Table 5 presents statistical results for the first analysis of the numerical experiments where all independent runs reached a feasible solution.

Based on the performance obtained by CRPSO in the first analysis, it is used as the search algorithm in the second analysis.

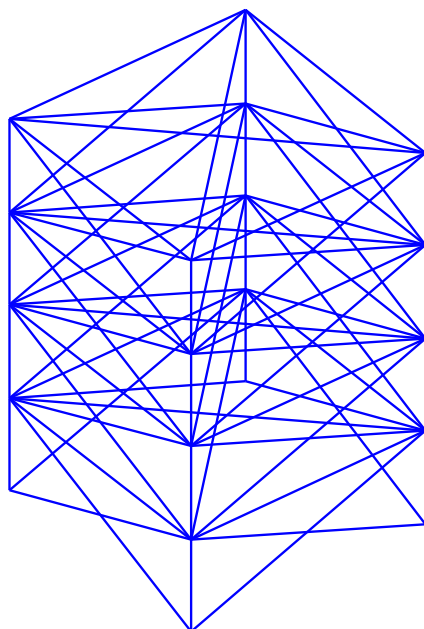


Fig. 26 The best result for the 72-bar truss with cardinality constraints for $m = 1$

6.1 The second set of numerical experiments

The second analysis refers to the use the CRPSO to solve the optimization problems considering cardinality constraints to find the best member groupings. The results for the best solutions are presented in Table 6, 7, 8 and 9 where dv means design variable, nfe is the number of maximum function evaluations, m is the cardinality constraint and “no c.c.” indicates no cardinality constraints. Just after the label “no c.c.” appears the number of distinct cross-sectional areas found when no cardinality constraint was set.

Table 6 presents the results for the 10-bar truss. Figure 8 shows the best configuration when no cardinality constraints are adopted. Figures 9, 10, 11 and 12 show the best configurations considering $m = 1, 2, 3$ and 4, respectively, and each color represents a distinct cross-sectional area.

The results for the 37-bar truss are presented in Table 7. Figure 13 shows the best result without cardinality constraint whereas Figs. 14, 15, 16 and 17 present the best results considering cardinality constraints for $m = 1, 2, 3, 4$, respectively.

The obtained results for the 52-bar truss dome are shown in Table 8. Figures 18, 19 and 20 show the best results without cardinality constraints whereas Figs. 21, 22, 23 and 24 show the best results considering cardinality constraints.

The best results with and without cardinality constraints for the 72-bar truss are presented in Table 9. Figure 25 presents the best solution without cardinality constraints whereas Figs. 26, 27, 28 and 29 show the best results considering cardinality constraints.

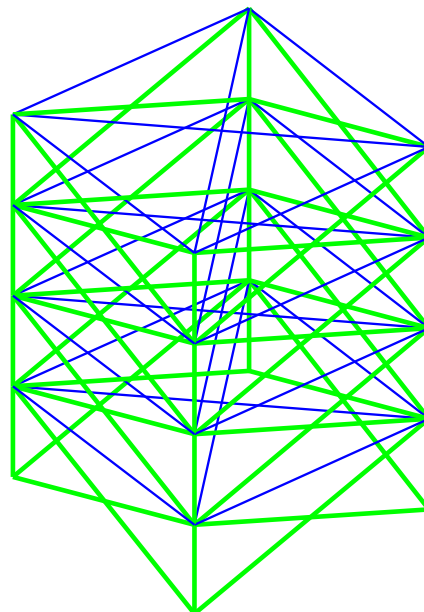


Fig. 27 The best result for the 72-bar truss with cardinality constraints for $m = 2$

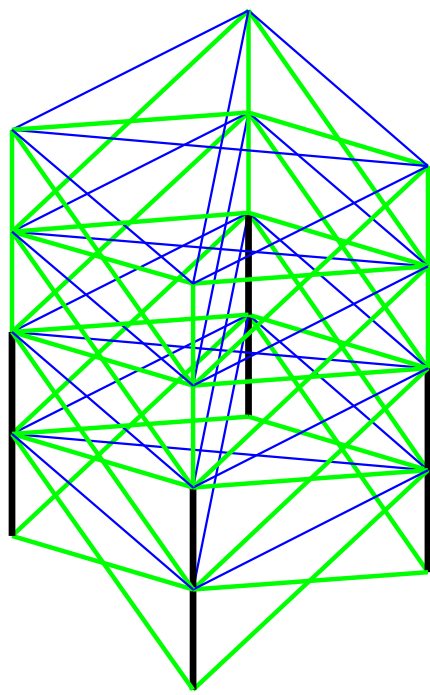


Fig. 28 The best result for the 72-bar truss with cardinality constraints for $m = 3$

Figures 30, 31, 32 and 33 show tradeoff between weight and number of sections for the 10-, 37-, 52- and 72-bar trusses between the final weights and the number of distinct cross-sectional areas. One can observe the weight reduction as the number of distinct cross-sectional areas increases.

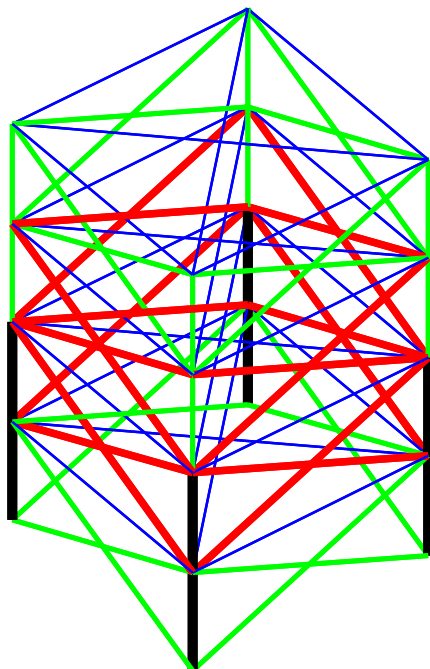


Fig. 29 The best result for the 72-bar truss with cardinality constraints for $m = 4$

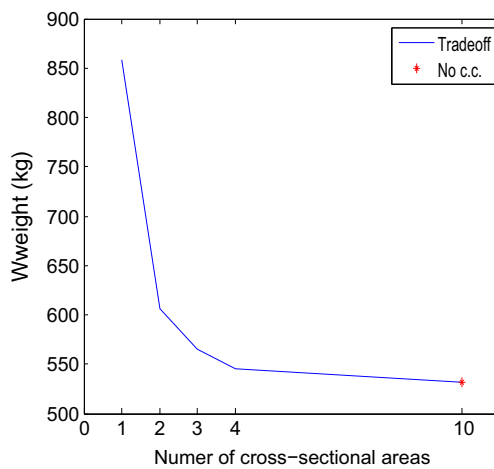


Fig. 30 The tradeoff between the final weight and the number of cross-sectional areas for the 10-bar truss

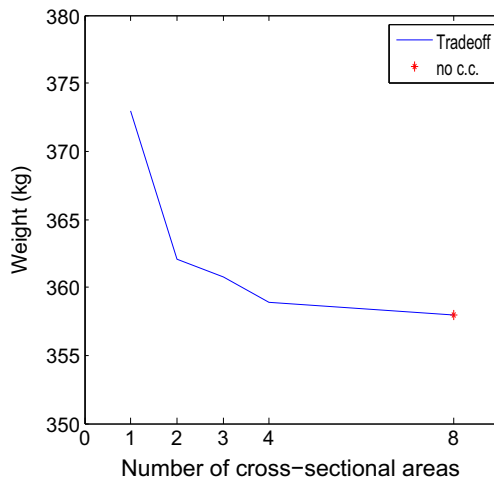


Fig. 31 The tradeoff between the final weight and the number of cross-sectional areas for the 37-bar truss

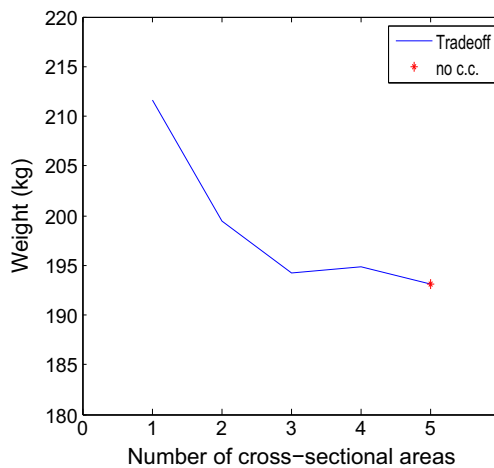


Fig. 32 The tradeoff between the final weight and the number of cross-sectional areas for the 52-nbar truss dome

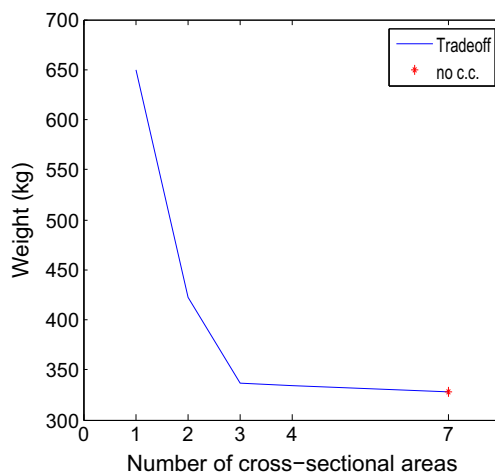


Fig. 33 The tradeoff between the final weight and the number of cross-sectional areas for the 72-bar truss

6.2 Additional experiment

In order to investigate more deeply these results obtained for the 52-bar truss dome an additional experiment, considering this example, was analyzed. The difference between the final weights (194.886, $m = 4$, and 194.276, $m=3$), is about 0.313 %. It can be happened since the special encoding considering $m = 4$ has a candidate particle in the CRPSO with a number of design variables greater than the case where $m = 3$ was set, consequently, making the search difficult. Also, this test-problem has continuous design variables such as the node coordinates, introducing more complexity in the problem. The new experiment considers the solution found where no cardinality was set (Last column of Table 8) maintaining the node coordinates fixed (the same reached in this solution). In this way, the 52-bar truss dome, presenting only sizing design variables, was submitted to cardinality constraints. The results are presented in Table 10.

Table 10 Additional results for the 52-bar truss, where areas A_i are in cm^2 and the node coordinates X_i and Z_i are in meters

dv	$m = 1$	$m = 2$	$m = 3$	$m = 4$	no c.c. (5)
A_1-A_4	1.5	1.2	1.0	1.0	1.0
A_5-A_8	1.5	1.2	1.3	1.3	1.3
A_9-A_{16}	1.5	1.2	1.3	1.3	1.3
$A_{17}-A_{20}$	1.5	1.5	1.5	1.5	1.6
$A_{21}-A_{28}$	1.5	1.5	1.3	1.3	1.4
$A_{29}-A_{36}$	1.5	1.2	1.0	1.0	1.0
$A_{37}-A_{44}$	1.5	1.5	1.5	1.5	1.5
$A_{45}-A_{52}$	1.5	1.5	1.5	1.5	1.4
Natural frequencies					
f_1 (Hz)	13.757673	13.653104	12.944006	28.661781	12.808075
f_2 (Hz)	29.260660	28.720916	28.661781	12.944006	28.659108
W (kg)	217.345059	209.050297	193.829759	193.829759	193.588995
nfe	24000	24000	24000	24000	24000

Observing the solutions found for $m = 3$ and $m = 4$ are exactly the same and it is possible to conclude that the best member grouping prefers to use only three different areas than four different areas. This may be due to a particular feature of this optimization problem. Again, it is necessary to emphasize that there is a solution using 4 distinct cross-sectional areas with a final weight 0.313 % greater than the solution that uses 3 distinct cross-sectional areas as provided in Table 8.

6.3 Analysis of results – second set of numerical experiments

One can observe from Tables 6, 7, 8 and 9 and the tradeoff curves that the use of cardinality constraints provided very interesting results in the problems analyzed in this paper. As expected, when no cardinality constraint is adopted, the best weights were found. On the other hand, decreasing the cardinality constraint m , the final weights are increased. The tables and tradeoff curves provide a range of interesting solutions for the decision maker. The solutions are not conflicting, i.e., heavier structures with few distinct cross-sectional areas versus lighter structures with more distinct cross-sectional areas.

Tables 11, 12, 13 and 14 show the distinct cross-sectional areas, the weights and the percentage of each weight with respect to $m = 1$ and no c.c (last two columns), for 10-, 37-, 52- and 72-bar truss structures, respectively. The percentage of each weight with respect to $m = 1$ is determined by dividing a given weight by the weight when $m = 1$. For example, considering the 10-bar truss, 606.489 kg ($m = 2$) divided by 858.041 kg ($m = 1$) $\times 100\%$ is 70.68%. This percentage represents the gain obtained in the solutions increasing the cardinality constraint with respect to $m = 1$. One can observe from Table 11 that 10 distinct cross-sectional areas were found when no cardinality constraint

Table 11 Cross-sectional areas (in cm^2), weight (in kg) and the percentage of each weight with respect to $m = 1$ and no c.c. for the 37-bar truss

<i>m</i>								W		
1	29.0							858.041	100.00%	161.25%
2	38.6 13.0							606.489	70.68%	113.96%
3	42.6 20.6 6.7							565.448	65.90%	106.26%
4	40.7 20.8 11.8 4.3							545.226	63.54%	102.46%
no c.c.	35.5	35.4	24.5	24.4	14.5	14.4	12.8	12.3	4.7	0.645
								532.12	62.02%	100.00%

Table 12 Cross-sectional areas (in cm^2), weight (in kg) and the percentage of each weight with respect to $m = 1$ and no c.c. for the 37-bar truss

<i>m</i>								W		
1	1.9							372.966	100.00%	104.18%
2	2.3 1.4							362.031	97.07%	101.12%
3	2.4 1.7 1.1							360.754	96.73&	100.77%
4	2.9 2.7 1.3 1.0							358.856	96.22%	100.24%
no c.c.	3.0	2.7	2.6	2.5	1.6	1.3	1.2	1.0	358.007	95.99%
										100.00%

Table 13 Cross-sectional areas (in cm^2), weight (in kg) and the percentage of each weight with respect to $m = 1$ and no c.c. for the 52-bar truss

<i>m</i>								W		
1	1.5							211.605	100.00%	109.57%
2	1.5 1.0							199.504	94.28%	103.30%
3	1.5 1.4 1.0							194.276	91.81%	100.59%
4	1.6 1.4 1.2 1.0							194.886	92.10%	100.91%
no c.c.	1.7	1.4	1.3	1.2	1.0			193.131	91.27%	100.00%

Table 14 Cross-sectional areas (in cm^2), weight (in kg) and the percentage of each weight with respect to $m = 1$ and no c.c. for the 72-bar truss

<i>m</i>								W		
1	10.8							649.596	100.00%	197.92%
2	11.0 0.645							422.328	65.01%	128.67%
3	14.4 8.1 0.645							336.238	51.76&	102.44%
4	14.7 8.4 7.7 0.645							334.386	51.48%	101.88%
no c.c.	16.8	13.1	8.3	8.0	7.9	3.7		328.215	50.53%	100.00%

Table 15 Statistical results and computational time for the numerical experiments

	Best	Median	Average	Std	Worst	Time (s)
10-bar truss						
$m = 1$	858.041	858.041	858.041	0.000	858.041	54
$m = 2$	606.489	606.489	626.298	25.832	691.269	56
$m = 3$	565.447	595.060	592.903	20.554	666.980	56
$m = 4$	545.226	583.143	579.173	16.961	623.270	56
no c.c.	532.123	539.490	539.755	6.055	556.849	56
37-bar truss						
$m = 1$	372.966	372.984	373.421	1.251	379.653	236
$m = 2$	362.031	367.921	367.930	2.818	373.341	262
$m = 3$	360.754	365.880	365.871	2.653	372.966	254
$m = 4$	358.856	364.702	364.597	2.728	369.810	244
no c.c.	358.007	359.504	361.347	5.066	381.234	231
52-bar truss dome						
$m = 1$	211.605	211.612	214.618	5.407	224.270	344
$m = 2$	199.501	208.943	210.527	8.098	245.351	345
$m = 3$	194.275	205.523	207.069	6.085	227.206	357
$m = 4$	194.886	205.831	207.435	6.753	224.269	362
no c.c.	193.130	200.187	207.885	31.060	376.887	313
72-bar truss						
$m = 1$	649.596	649.596	649.596	0.000	649.596	456
$m = 2$	422.328	507.841	498.827	29.434	564.028	488
$m = 3$	336.238	410.799	416.624	52.952	513.087	486
$m = 4$	334.386	375.900	388.106	42.102	513.087	494
no c.c.	328.214	328.364	332.722	29.469	378.978	439

Table 16 New member grouping for each truss

	10-bar truss
Group 1	A ₁ ,A ₃
Group 2	A ₂ ,A ₉ ,A ₁₀
Group 3	A ₄ ,A ₇ ,A ₈
Group 4	A ₅ ,A ₆
	37-bar truss
Group 1	A ₁ ,A ₄ ,A ₁₀ ,A ₁₃ ,A ₁₆ ,A ₁₉ ,A ₂₅ ,A ₂₇
Group 2	A ₂ ,A ₆ ,A ₈ ,A ₉ ,A ₁₁ ,A ₁₂ ,A ₁₅ ,A ₁₇ ,A ₁₈ ,A ₂₀ ,A ₂₁ ,A ₂₆
Group 3	A ₃ ,A ₅ ,A ₁₄ ,A ₂₃ ,A ₂₄
Group 4	A ₇ ,A ₂₂
	52-bar truss dome
Group 1	A ₁ -A ₄ ,A ₂₉ -A ₃₆
Group 2	A ₅ -A ₈ ,A ₁₇ -A ₂₀
Group 3	A ₉ -A ₁₆ ,A ₂₁ -A ₂₈ ,A ₄₅ -A ₅₂
Group 4	A ₃₇ -A ₄₄
	72-bar truss
Group 1	A ₁ -A ₄ ,A ₅ -A ₁₂ ,A ₁₉ -A ₂₂ ,A ₅₉ -A ₆₆
Group 2	A ₁₃ -A ₁₆ ,A ₁₇ -A ₁₈ ,A ₃₁ -A ₃₄ ,A ₃₅ -A ₃₆ ,A ₄₉ -A ₅₂ ,A ₅₃ -A ₅₄ ,A ₆₇ -A ₇₀ ,A ₇₁ -A ₇₂
Group 3	A ₂₃ -A ₃₀ ,A ₄₁ -A ₄₈
Group 4	A ₃₇ -A ₄₀ ,A ₅₅ -A ₅₈ ,

was set, leading to a final weight of 532.124 kg. On the other hand, setting $m = 4$, only 4 distinct cross-sectional areas were found, leading to a final weight of 545.226 kg, 2.46% heavier with respect to the case when no cardinality constraint was set. Clearly, the choice by solution $m = 4$ is much more interesting in comparison when no cardinality constraint is set. On the other hand the last line of Tables 11 to 14 indicates 100% for the weight obtained when no cardinality constraint was set and the relative percentage of the others solutions when $m = 1, 2, 3$ and 4. For example, when $m = 1$ the final weight is 61.25% greater than the final weight obtained when no cardinality constraint was set.

The results for the 37-bar truss presented in Table 12 indicate that the gain in terms of percentage of weight is not significant among the solutions. Setting $m = 3$ or 4, all of the solutions are competitive. It is important to note that this problem has sizing (discrete) and shape (continuous) design variables. The solution without cardinality constraints set 8 distinct cross-sectional areas presenting a final weight equal to 358.007 kg and setting $m = 4$ a final weight equal to 358.856 kg, 0.24% heavier, leading to a very interesting solution.

The results for the 52-bar truss dome presented in Table 13 show a competitiveness between the solutions when $m = 3$ and $m = 4$, 194.276 kg and 194.886 kg, respectively. In this case, setting $m = 4$ the final weight was worse than

Table 17 Results for the new member grouping of the experiments

dv	10-bar truss	37-bar truss	52-bar truss dome	72-bar truss
Group 1	39.9	2.7	1.0	7.9
Group 2	12.6	1.3	1.4	0.645
Group 3	20.2	1.0	1.4	8.2
Group 4	4.4	2.4	1.5	14.5
Z_1	—	—	5.461	—
X_2	—	—	2.154	—
Z_2	—	—	3.700	—
X_6	—	—	3.907	—
Z_6	—	—	2.500	—
$Y_{3,19}$	—	0.871	—	—
$Y_{5,17}$	—	1.249	—	—
$Y_{7,15}$	—	1.449	—	—
$Y_{9,13}$	—	1.602	—	—
Y_{11}	—	1.683	—	—
Natural frequencies				
f_1 (Hz)	7.000	20.001	12.872	4.000
f_2 (Hz)	18.449	40.000	28.648	—
f_3 (Hz)	20.001	60.001	—	6.006
W (kg)	543.615	358.326	193.603	334.386
nfe	14000	16000	16000	18000

Table 18 Statistical results for the new member grouping

	Best	Median	Average	Std	Worst
10-bar truss	543.615	544.036	544.594	2.589	559.948
37-bar truss	358.326	359.866	360.406	1.857	369.654
52-bar truss dome	193.603	195.359	198.686	5.316	216.918
72-bar truss	334.386	334.386	334.386	0.000	334.386

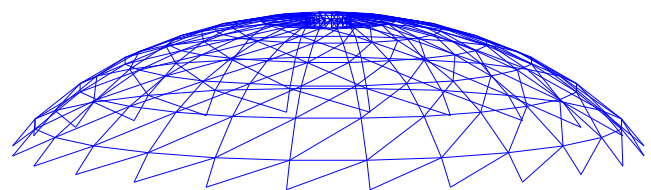


Fig. 34 Single layer 600-bar truss dome - 3d view

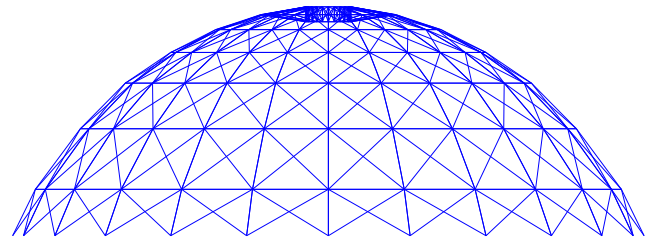


Fig. 35 Single layer 600-bar truss dome - side view

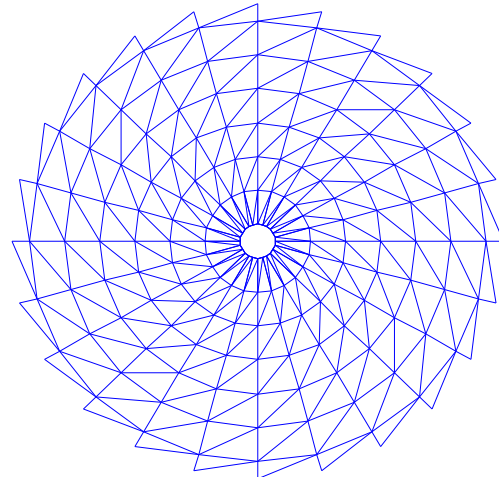


Fig. 36 Single layer 600-bar truss dome - top view

Table 19 Results for the 600-bar single layer dome truss, where areas A_i are in cm^2

dv	$m = 1$	$m = 2$	$m = 4$	$m = 6$	no c.c. (17)	(Kaveh and Ghazaan 2016)
A_1	10.5	7.5	14.0	7.0	1.5	1.0299
A_2	10.5	7.5	4.0	3.5	1.5	1.3664
A_3	10.5	16.5	7.5	6.0	7.0	5.1095
A_4	10.5	7.5	4.0	3.5	1.0	1.3011
A_5	10.5	7.5	14.0	15.5	16.5	17.0572
A_6	10.5	16.5	18.0	34.5	34.5	34.0764
A_7	10.5	16.5	18.0	15.5	12.0	13.0985
A_8	10.5	7.5	18.0	15.5	15.5	15.5882
A_9	10.5	16.5	14.0	15.5	10.5	12.6889
A_{10}	10.5	7.5	7.5	15.5	10.0	10.3314
A_{11}	10.5	16.5	7.5	7.0	8.5	8.5313
A_{12}	10.5	16.5	7.5	7.0	9.0	9.8308
A_{13}	10.5	7.5	7.5	7.0	7.5	7.0101
A_{14}	10.5	7.5	4.0	6.0	5.5	5.2917
A_{15}	10.5	7.5	7.5	7.0	6.5	6.2750
A_{16}	10.5	7.5	7.5	7.0	5.5	5.4305
A_{17}	10.5	7.5	4.0	3.5	5.0	3.6414
A_{18}	10.5	7.5	14.0	6.0	7.5	7.2827
A_{19}	10.5	7.5	4.0	3.5	4.5	4.4912
A_{20}	10.5	7.5	4.0	3.5	2.0	1.9275
A_{21}	10.5	7.5	7.5	3.5	4.5	4.6958
A_{22}	10.5	7.5	4.0	7.0	4.0	3.3595
A_{23}	10.5	7.5	4.0	3.5	2.0	1.7067
A_{24}	10.5	7.5	4.0	7.0	4.5	4.8372
A_{25}	10.5	7.5	4.0	7.0	1.5	2.0253
Natural frequencies						
f_1 (Hz)	6.469789	5.823299	5.786822	5.749498	5.023073	5.001306
f_3 (Hz)	7.008522	7.013624	7.015862	7.002091	7.001284	7.004924
W (kg)	10589.847087	8745.706063	7594.071137	7285.017517	6132.295854	6175.33
nfe	1600	3200	6400	9600	20000	20000

when $m = 3$, i.e., 0.31% heavier. This is not a considerable difference and the solutions are very competitive.

Observing the results presented in Table 14 for the 72-bar truss, the gain is considerable when m is increased. Comparing the solutions when $m = 4$ (334.886 kg, using 4

distinct cross-sectional areas) and when no cardinality constraint was set (328.215 kg, using 7 distinct cross-sectional areas) the percentage difference between the final weights is 1.88%. The solution with $m = 4$ can be a good solution for the decision maker.

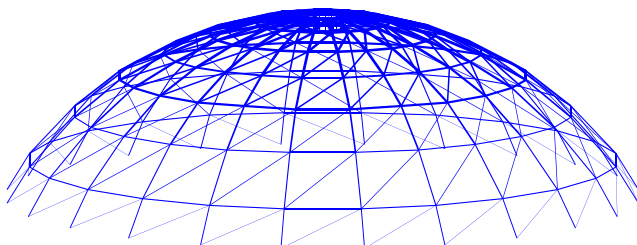


Fig. 37 The best result for the 600-bar truss dome without cardinality constraints - 3D view

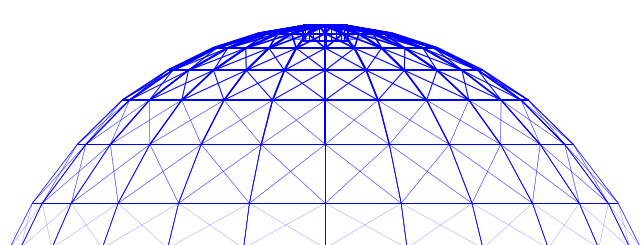


Fig. 38 The best result for the 600-bar truss dome without cardinality constraints - side view

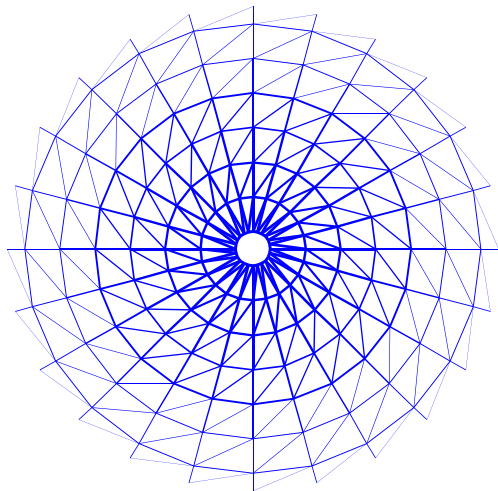


Fig. 39 The best result for the 600-bar truss dome without cardinality constraints - top view

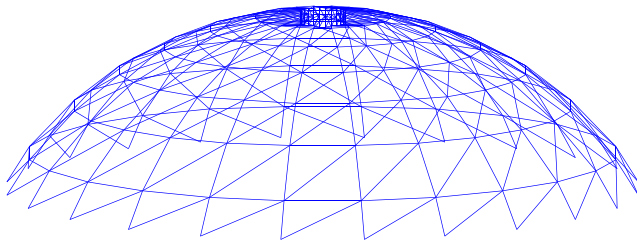


Fig. 40 The best result for the 600-bar truss dome with cardinality constraints for $m = 1$ - 3d view

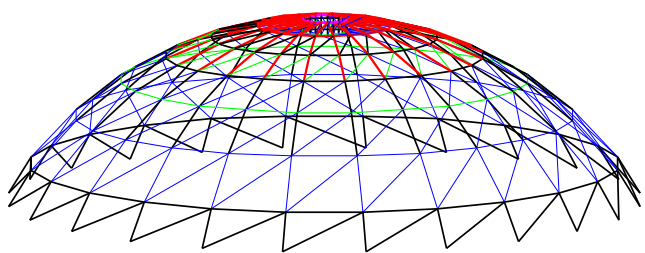


Fig. 43 The best result for the 600-bar truss dome with cardinality constraints for $m = 6$ - 3d view

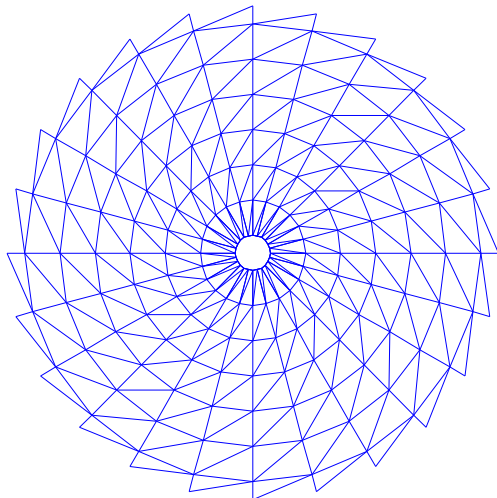


Fig. 44 The best result for the 600-bar truss dome with cardinality constraints for $m = 1$ - top view

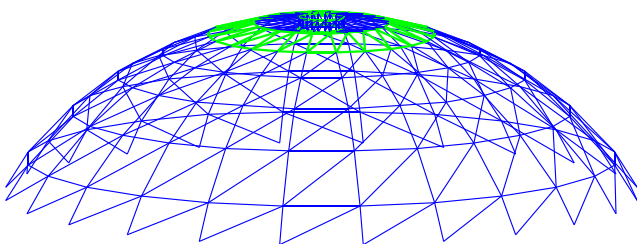


Fig. 41 The best result for the 600-bar truss dome with cardinality constraints for $m = 2$ - 3d view

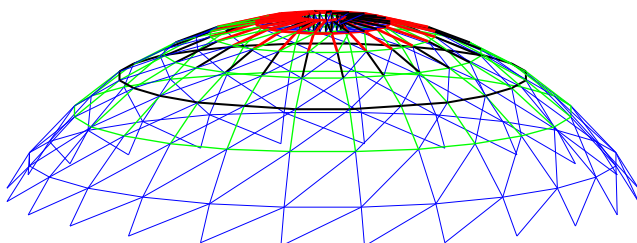


Fig. 42 The best result for the 600-bar truss dome with cardinality constraints for $m = 4$ - 3d view

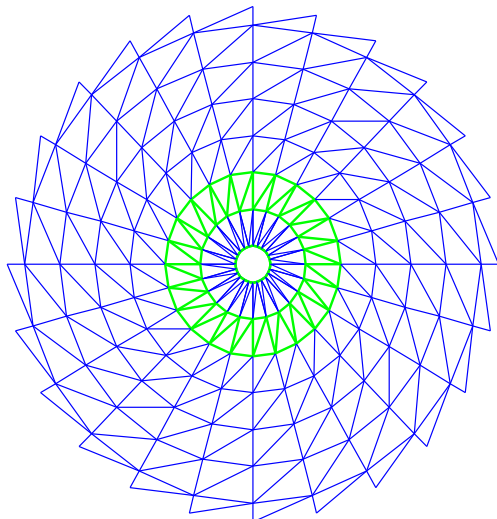


Fig. 45 The best result for the 600-bar truss dome with cardinality constraints for $m = 2$ - top view

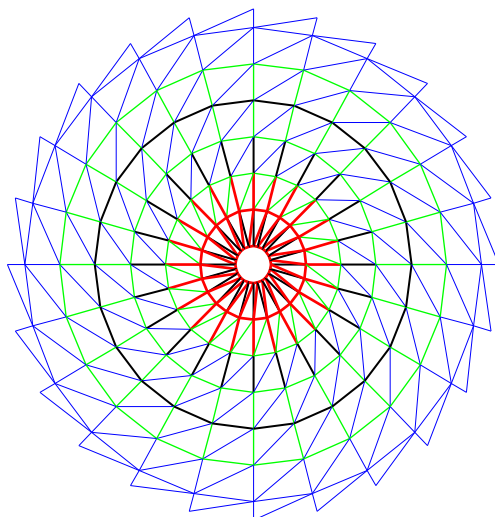


Fig. 46 The best result for the 600-bar truss dome with cardinality constraints for $m = 4$ - top view

A well-defined or uniform search space (with one or two significant digits after the comma), for the sizing design variables adopted here, from (Kaveh et al. 2015a), certainly, provides expected results and one can consider them coherent with the value of the given cardinality constraints. In this sense, the weights decreases when the cardinality m increase.

A final, and important, finding relates to the number of sizing design variables originally defined for each problem (10 for the 10-bar truss, 14 for the 37 bar-truss, 8 for the 52-bar truss dome and 16 for the 72-bar truss). From the results obtained in the numerical experiments conducted in this paper, new member groups were automatically defined.

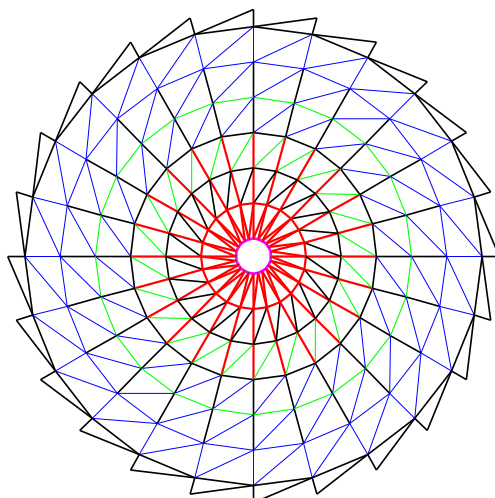


Fig. 47 The best result for the 600-bar truss dome with cardinality constraints for $m = 6$ - top view

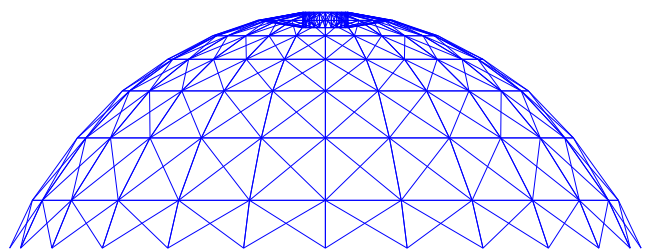


Fig. 48 The best result for the 600-bar truss dome with cardinality constraints for $m = 1$ - side view

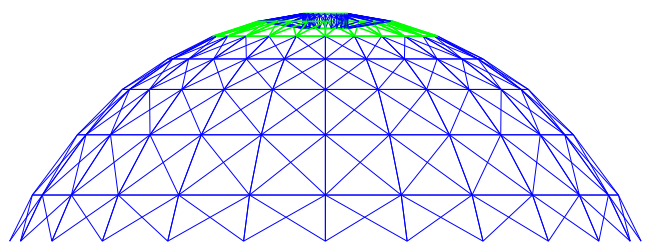


Fig. 49 The best result for the 600-bar truss dome with cardinality constraints for $m = 2$ - side view

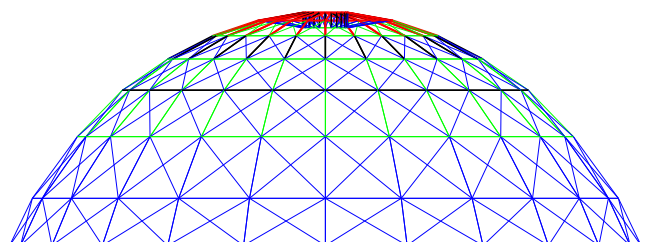


Fig. 50 The best result for the 600-bar truss dome with cardinality constraints for $m = 4$ - side view

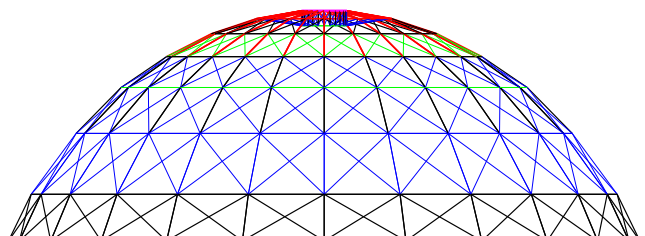


Fig. 51 The best result for the 600-bar truss dome with cardinality constraints for $m = 6$ - side view

Fig. 52 Double layer 1410-bar truss dome - 3d view

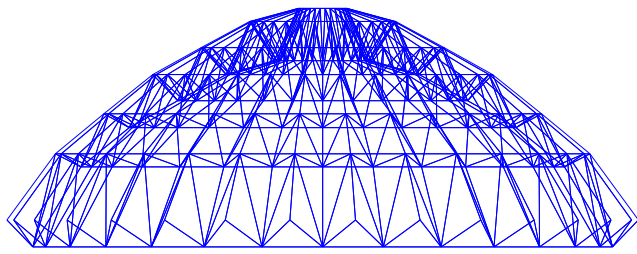
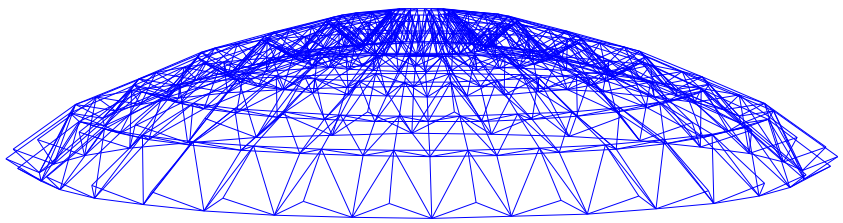


Fig. 53 Double layer 1410-bar truss dome - side view

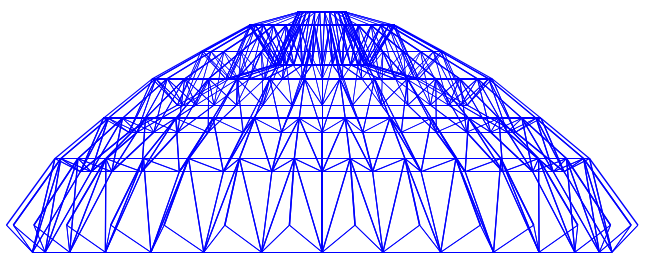


Fig. 56 The best result for the 1410-bar truss dome without cardinality constraints - side view

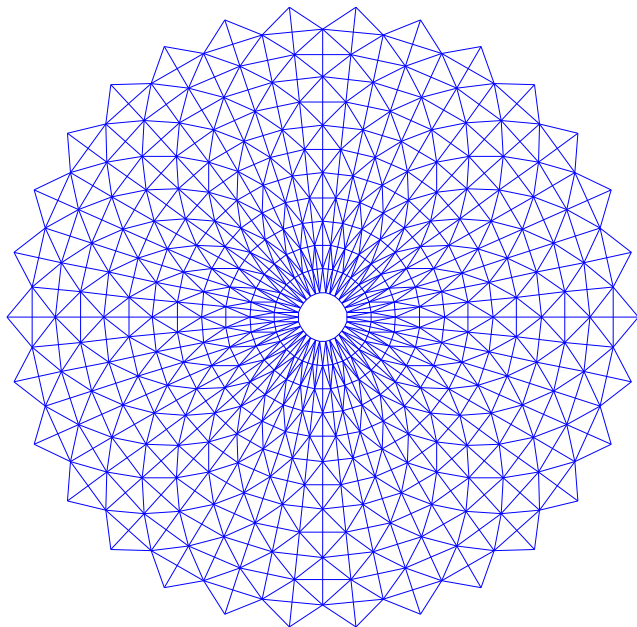


Fig. 54 Double layer 1410-bar truss dome - top view

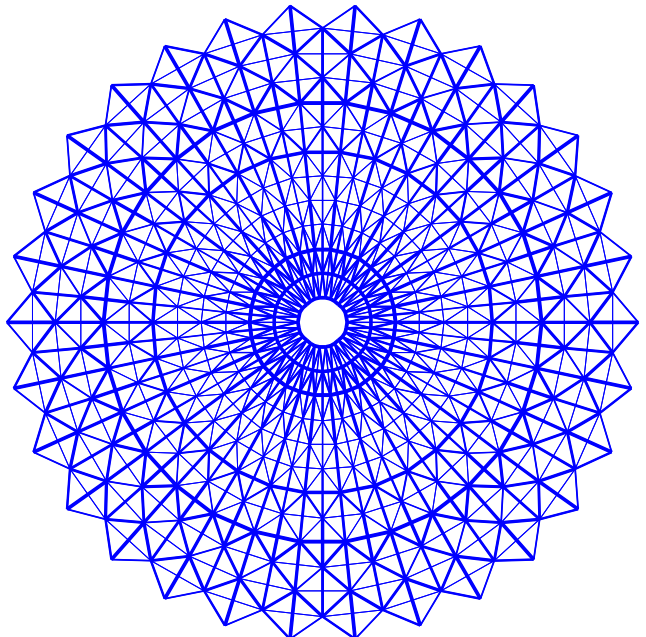


Fig. 57 The best result for the 1410-bar truss dome without cardinality constraints - top view

Fig. 55 The best result for the 1410-bar truss dome without cardinality constraints - 3D view

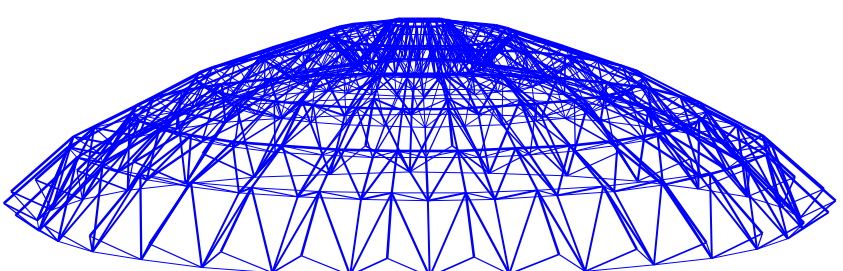


Table 20 Results for the 1410-bar double layer dome truss, where areas A_i are in cm^2

dv	$m = 1$	$m = 2$	$m = 4$	$m = 6$	no c.c. (22)	(Kaveh and Ghazaan 2016)
A_1	11.5	11.5	5.5	4.5	2.5	7.9969
A_2	11.5	11.5	5.5	4.5	6.0	6.1723
A_3	11.5	11.5	19.5	14.0	18.0	35.5011
A_4	11.5	11.5	9.5	8.5	9.5	10.2510
A_5	11.5	3.5	5.5	3.0	6.0	5.3727
A_6	11.5	3.5	1.5	3.0	1.0	1.3488
A_7	11.5	11.5	19.5	12.0	29.5	11.4427
A_8	11.5	11.5	9.5	8.5	8.0	9.7157
A_9	11.5	3.5	1.5	4.5	2.0	1.3005
A_{10}	11.5	3.5	5.5	3.0	1.5	2.5046
A_{11}	11.5	11.5	9.5	14.0	1.0	10.7849
A_{12}	11.5	11.5	5.5	8.5	7.5	10.1954
A_{13}	11.5	3.5	5.5	4.5	1.0	2.2300
A_{14}	11.5	3.5	9.5	4.5	6.0	5.1186
A_{15}	11.5	11.5	9.5	14.0	14.5	14.0053
A_{16}	11.5	11.5	5.5	8.5	9.0	8.9713
A_{17}	11.5	3.5	1.5	6.5	1.0	4.0756
A_{18}	11.5	3.5	5.5	4.5	8.0	5.9211
A_{19}	11.5	11.5	9.5	8.5	19.5	10.6915
A_{20}	11.5	11.5	19.5	14.0	16.5	10.6220
A_{21}	11.5	3.5	5.5	4.5	5.0	4.5064
A_{22}	11.5	11.5	9.5	14.0	9.0	8.4086
A_{23}	11.5	3.5	5.5	4.5	1.0	5.8405
A_{24}	11.5	11.5	5.5	4.5	5.0	5.0342
A_{25}	11.5	3.5	5.5	4.5	6.5	3.8932
A_{26}	11.5	11.5	5.5	4.5	5.5	6.1647
A_{27}	11.5	11.5	5.5	4.5	7.0	6.8990
A_{28}	11.5	11.5	19.5	4.5	15.5	11.6387
A_{29}	11.5	3.5	5.5	4.5	4.5	3.8343
A_{30}	11.5	3.5	5.5	3.0	2.5	1.4772
A_{31}	11.5	3.5	1.5	4.5	2.5	1.3075
A_{32}	11.5	3.5	5.5	6.5	1.0	4.4876
A_{33}	11.5	3.5	9.5	4.5	6.0	6.0196
A_{34}	11.5	3.5	1.5	3.0	1.0	2.6729
A_{35}	11.5	11.5	5.5	3.0	1.0	1.6342
A_{36}	11.5	3.5	5.5	4.5	1.0	1.8410
A_{37}	11.5	11.5	9.5	12.0	10.0	6.8841
A_{38}	11.5	3.5	5.5	4.5	5.5	4.1393
A_{39}	11.5	11.5	9.5	4.5	3.5	3.3264
A_{40}	11.5	3.5	1.5	4.5	1.0	1.0000
A_{41}	11.5	11.5	5.5	14.0	7.5	6.9376
A_{42}	11.5	3.5	5.5	4.5	8.5	4.4568

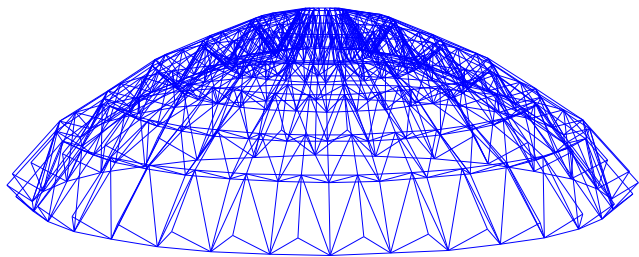
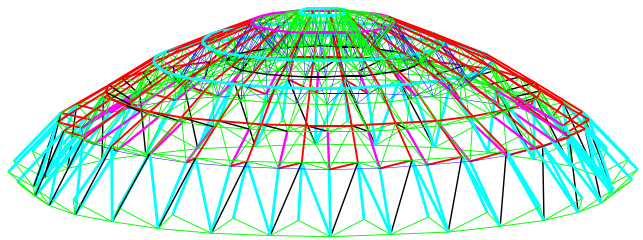
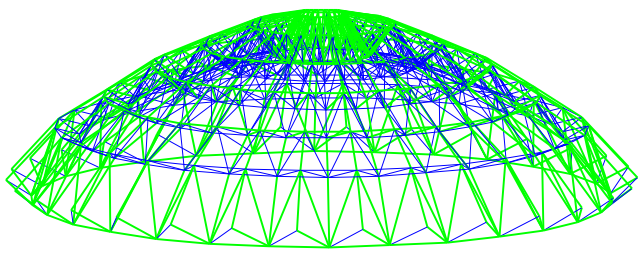
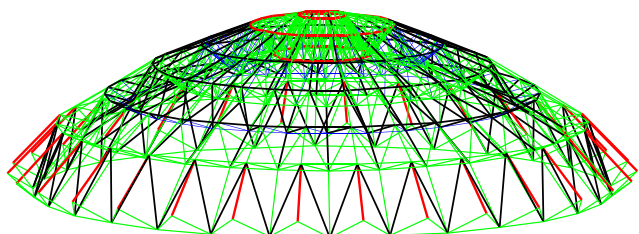
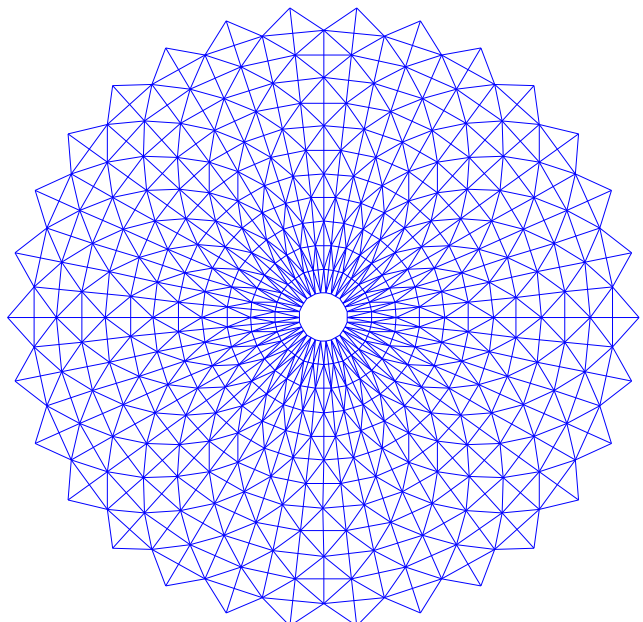
Table 15 presents the statistical analysis for the numerical experiments where “Std” means standard deviation, observing that all runs found feasible solutions. In this table is presented the computational time for one independent run for each experiment. The standard deviations increase as the

problems become more complex with the increase in the number of design variables.

Based on the results presented in Tables 6, 7, 8 and 9, one can observe that the automatic grouping of bars indicates a new member grouping of these bars for each experiment.

Table 21 Results for the 1410-bar double layer dome truss, where areas A_i are in cm^2 (continuation of Table 21)

dv	$m = 1$	$m = 2$	$m = 4$	$m = 6$	no c.c.	(Kaveh and Ghazaan 2016)
A_{43}	11.5	3.5	5.5	8.5	7.5	4.6758
A_{44}	11.5	11.5	5.5	3.0	1.0	1.0084
A_{45}	11.5	3.5	9.5	6.5	7.5	7.5103
A_{46}	11.5	3.5	5.5	4.5	6.5	5.2449
A_{47}	11.5	11.5	5.5	4.5	1.0	1.0550
Natural frequencies						
f_1 (Hz)	8.618764	7.085395	7.036309	7.002220	7.000774	7.002
f_3 (Hz)	9.089049	9.011212	9.004514	9.015927	9.006830	9.001
W (kg)	20803.265478	13634.047654	12265.176396	11796.365748	11044.616778	10504.20
nfe	1600	3200	6400	9600	20000	20000

**Fig. 58** The best result for the 1410-bar truss dome with cardinality constraints for $m = 1$ - 3d view**Fig. 61** The best result for the 1410-bar truss dome with cardinality constraints for $m = 6$ - 3d view**Fig. 59** The best result for the 1410-bar truss dome with cardinality constraints for $m = 2$ - 3d view**Fig. 60** The best result for the 1410-bar truss dome with cardinality constraints for $m = 4$ - 3d view**Fig. 62** The best result for the 1410-bar truss dome with cardinality constraints for $m = 1$ - top view

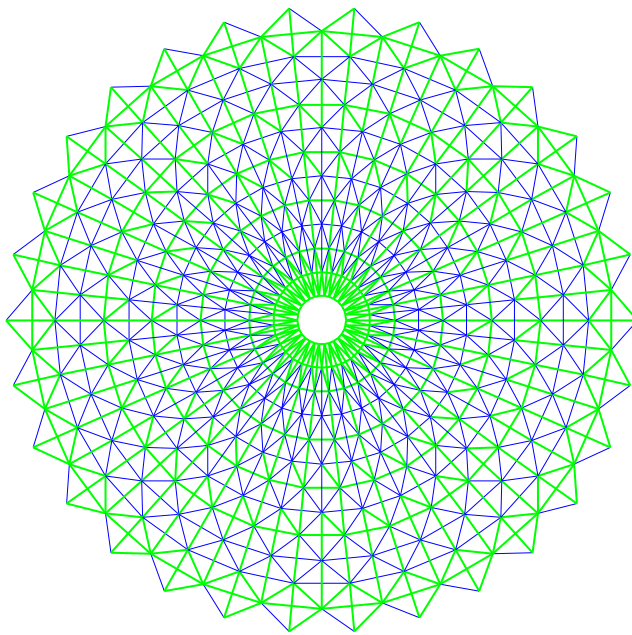


Fig. 63 The best result for the 1410-bar truss dome with cardinality constraints for $m = 2$ - top view

The results were competitive for $m = 4$ with respect to the case with no cardinality constraint, that is, the difference between the final weights was very small in these cases. Thus, in order to evaluate the performance of these new groups, new tests were performed considering the new groups obtained from the case when $m = 4$.

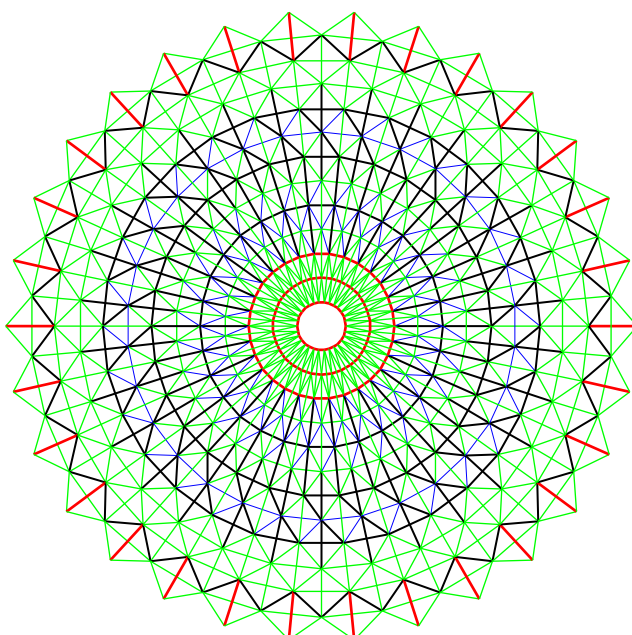


Fig. 64 The best result for the 1410-bar truss dome with cardinality constraints for $m = 4$ - top view

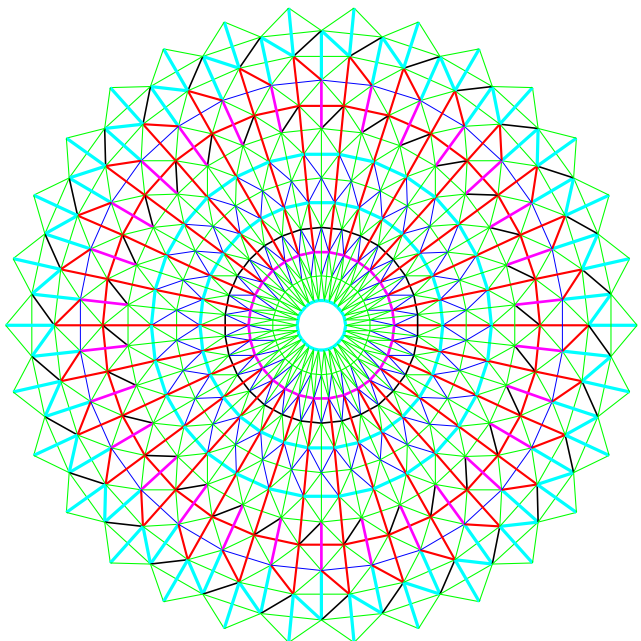


Fig. 65 The best result for the 1410-bar truss dome with cardinality constraints for $m = 6$ - top view

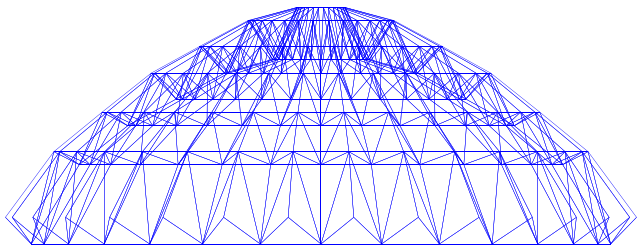


Fig. 66 The best result for the 1410-bar truss dome with cardinality constraints for $m = 1$ - side view

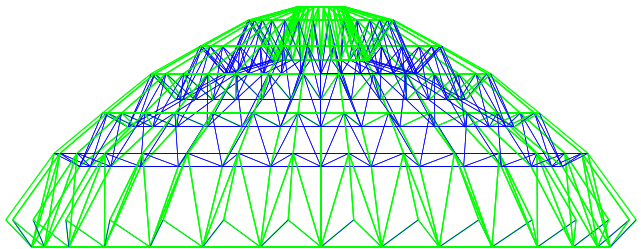


Fig. 67 The best result for the 1410-bar truss dome with cardinality constraints for $m = 2$ - side view

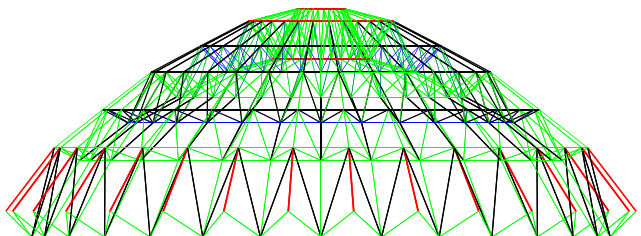


Fig. 68 The best result for the 1410-bar truss dome with cardinality constraints for $m = 4$ - side view

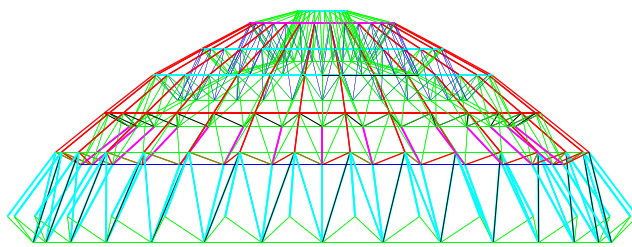


Fig. 69 The best result for the 1410-bar truss dome with cardinality constraints for $m = 6$ - side view

Table 16 shows the new member grouping for each experiment and the results for the new member grouping are shown in Table 17. The statistical analysis for the numerical experiments for the new member grouping are presented in Table 18.

Observing the results presented in Table 17 one can conclude that they are very competitive with those obtained with the original groups. For the 10-bar truss the new group achieved 543.615 kg in comparison with 532.124 kg (2.15% heavier). For the 37-bar the new group found 358.326 kg against 358.007 kg (0.09% heavier). For the 52-bar truss dome 193.603 kg against 193.131 kg (0.24% heavier), and, finally, for the 72-bar truss 334.386 kg versus 328.215 kg (1.88% heavier). In addition to the results presented for the new member grouping being competitive compared to the original group, it is important to highlight another advantage of the new grouping with respect to the number of function evaluations of the objective function. For all experiments only 2/3 of the budget was used in the analyzes. Also, for all examples using the new member grouping the results are equal or better than those found when m was set equal to 4.

7 The third set of numerical experiments

In order to handle large scale problems, the third set of numerical experiments analyses a 600-bar single layer dome truss and a 1410-bar double layer dome truss defined in Kaveh and Ghazaan (2016). Unlike the reference (Kaveh

and Ghazaan 2016), which uses a continuous search space, discrete search spaces are adopted considering the same limits of these continuous search spaces. In this section a 600-bar single layer and a 1410 double layer dome trusses are presented. The cardinality constraints are set equal to $m = 1$, $m = 2$, $m = 4$ and $m = 6$.

7.1 A 600-bar single layer dome truss

This example is presented in Kaveh and Ghazaan (2016) and Figures 34, 35 and 36 shows the views of the 600-bar single layer dome structure. The dome has 216 nodes and 600 elements and in reference (Kaveh and Ghazaan 2016) is possible to find a substructure in more detail for nodal numbering and coordinates. The dome has 13 meters of diameter and 7.5 meters of height. Each bar of this substructure is considered as a sizing design variable leading to a optimization problem with 25 variables. The elastic modulus is 200 GPa and the material density is 7850 kg/m^3 and the nodes at the bottom of the dome (coordinates $z = 0$), are completely restricted. A non-structural mass of 100 kg is added at all free nodes. The discrete search space for this problem is defined in the range $1.0, 1.5, 2.0, 2.5, 3.0, \dots, 99.0, 99.5$ and 100 cm^2 . The limits for the natural frequencies are $f_1 \geq 5 \text{ Hz}$ and $f_2 \geq 7 \text{ Hz}$.

Table 19 shows the results for the case where the cardinality constraints were set equal to $m = 1$, $m = 2$, $m = 4$, $m = 6$ and no cardinality constraints. Figures 37, 38 and 39 show the best result for the 600-bar truss dome without cardinality constraints. Figures from 40, 41, 42, 43, 44, 45, 46, 47, 48, 49, 50 and 51 show the final designation of the cross-sectional areas for each case ($m = 1$, $m = 2$, $m = 4$, $m = 6$).

7.2 A 1410-bar double layer dome truss

A 1410-bar double layer dome truss is depicted in Figs. 52, 53 and 54 is composed of 390 nodes and 1410 elements. As in the 600-bar single layer dome truss test problem, in reference (Kaveh and Ghazaan 2016) is possible to find a substructure in more details for nodal

Table 22 Cross-sectional areas (in cm^2), weight (in kg) and the percentage of each weight with respect to $m = 1$ and no c.c. for the 600-bar single layer dome

Table 23 Cross-sectional areas (in cm²), weight (in kg) and the percentage of each weight with respect to $m = 1$ and no c.c. for the 1410-bar double layer dome truss

<i>m</i>	W											
1	11.5											
2	11.5 3.5											
4	19.5 9.5 5.5 1.5											
6	14.0 12.0 8.5 6.5 4.5 3.0											
no c.c.	29.5 19.5 18.0 16.5 15.5 14.5 10.0 9.5 9.0 8.5 8.0											
	7.5 7.0 6.5 6.0 5.5 5.0 4.5 3.5 2.5 1.5 1.0											
	11044.616											
	53.09%											
	100.00%											

numbering and coordinates. The dome has 13 meters of outer diameter and 4.5 meters of height. The total number of sizing design variable is equal to 47 variables. The elastic modulus is 200 GPa and the material density is 7850 kg/m³. A non-structural mass of 100 kg is attached to all free nodes and the discrete search space is defined by the following cross-sectional areas 1.0, 2.0, 3.0, 4.9, 5.0 · .. 95.0, 96.0, 97.0, 98.0, 99.0 and 100 cm². The limits for the natural frequencies are $f_1 \geq 7$ Hz and $f_3 \geq 9$ Hz.

Table 20 and 21 show the results for the case where the cardinality constraints were set equal to $m = 1$, $m = 2$, $m = 4$, $m = 6$ and no cardinality constraints. Figures 55, 56 and 57 show the best results for 1410-bar truss without cardinality constraints, 3D, side and top views, respectively. Figures from 58, 59, 60, 61, 62, 63, 64, 65, 66, 67, 68 and 69 show the final designation of the cross-sectional areas for each case ($m = 1$, $m = 2$, $m = 4$, $m = 6$).

7.3 Analysis of results – third set of numerical experiments

The results provided in Tables 19, 20 and 21 show to be able to handle large-scale structural optimization problems. When no cardinality constraints were set the results

found in both cases were very competitive or better than those presented in Kaveh and Ghazaan (2016). For the 600-bar single layer dome truss a final weight equal to 6132.29 kg (discrete search space) against 6175.33 (continuous search space). For the 1410-bar double layer dome truss 11044.616 kg (discrete search space) against 10504.20 (continuous search space). In the both experiments the number of function evaluations was the same adopted in Table 21.

Considering cardinality constraints to find the best member groupings, the results found in the analyses show to be coherent. As in the second set of numerical experiments m grows the weight decreases. The results for the the 600-bar single layer dome truss can be considered reasonable. For instance, using only 6 distinct cross-sectional areas the final weight was equal to 7285.017 kg against 6132.295 kg, using 17 distinct cross-sectional areas. The difference between the final weights is only 18.80%. In particular, the results obtained for 1410-bar double layer dome truss were quite interesting. One can observe that setting $m = 6$, using only 6 different cross-sectional areas, the final weight was equal to 11044.616 kg against 10504.20 kg obtained with 22 different areas, with no cardinality constraints. The difference between the final weights is only 5.14%.

Table 24 Statistical results and computational time for the large-scale set of experiments

	Best	Median	Average	Std	Worst	Time (s)
600-bar truss dome						
$m = 1$	10589.847087	10589.847087	10589.847087	0	10589.847087	328
$m = 2$	8745.706063	9637.836036	9646.707398	534.720121	10589.847087	578
$m = 4$	7594.071137	8833.853862	8804.100298	637.660037	10137.431331	1099
$m = 6$	7285.017517	8515.689869	8566.912883	516.654059	9871.140386	1782
no c.c.	6132.295854	6300.092639	6682.319163	999.245846	10409.940679	3390
1410-bar truss dome						
$m = 1$	20803.265478	20803.265478	20803.265478	0	20803.265478	814
$m = 2$	13634.047654	15080.365195	15402.732303	1375.524175	18767.772745	1735
$m = 4$	12265.176396	13507.116915	13498.645336	760.728285	15431.389989	3143
$m = 6$	11796.365748	12898.147512	1285.607123	657.733480	14356.422214	5212
no c.c.	11044.616778	12694.310952	13017.899563	1454.812976	15496.852679	9900

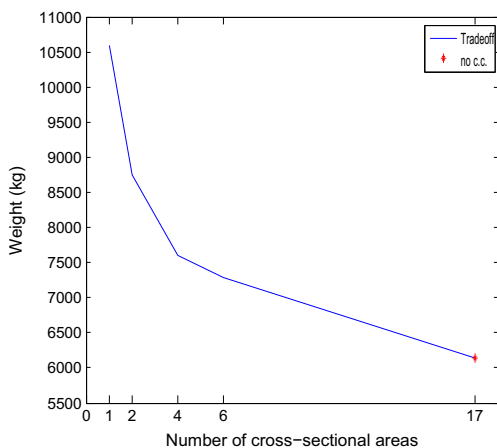


Fig. 70 The tradeoff between weight and number of sections for the 600-bar truss dome

These experiments can be considered with high complexity when submitted to weight minimization setting multiple natural frequencies as constraints. Hence, it was expected great values of standard deviations as can be observed from these metrics presented in Table 24, except to the case when $m = 1$.

Tables 22 to 23 show the distinct cross-sectional areas, the weights and the percentage of each weight with respect to $m = 1$ and no c.c (last two columns), for the 600-bar single layer dome and 1410-bar double layer dome truss structures, respectively.

Table 24 presents the statistical results and computational time for the large-scale set of experiments. Figures 70 and 71 show tradeoff between weight and number of sections for 600 single layer and 1410 double layer dome trusses, respectively, between the final weights and the number of distinct cross-sectional areas. Again, it is possible

to observe the weight reduction as the number of distinct cross-sectional areas increases.

8 Conclusions and future work

The structural optimization problems analyzed in this paper are widely discussed in the literature. Two of them have only sizing design variables (10- and 72-bar trusses), and the others (37-bar truss and 52-bar truss dome), have sizing and shape design variables.

The numerical experiments analyzed in this paper can be considered a new test-bed for the literature with respect to new member groups for the benchmark problems analyzed here. It is justified by the use of cardinality constraints to discover member groupings as well as the use of discrete or mixed (discrete/continuous) search spaces in the formulations of the structural optimization problems with multiple natural frequencies as constraints.

The advantages of discovering new member grouping can be justified, for instance, in the fabrication of transmission towers to cover a very long distance. It can lead to economy in fabrication, checking, transportation and so on, using a reduced number of distinct cross-sectional areas. For example, one can think in to reduce the fabrication costs when setting in the machine to laminate few items accelerating the production costs leading to economies in final cost of the profiles. Also, it is expected a labor-saving when the structure is welded, checked and so on.

A discrete search space for sizing design variables, maintaining the continuous search space for shape design variables, is used here. It is important to note that the robustness of the proposed strategy in discovering desirable member grouping by using cardinality constraints and using a coarser discrete search space as well as a continuous search space will be analyzed in future works. Previous works in this sense can be checked in the references (Barbosa et al. 2008; Lemonge et al. 2011a).

The new member grouping proposed in this paper for the structures analyzed here is going to be tested considering continuous search spaces. New member grouping are proposed from the results obtained when cardinality constraints were considered and they can be used for reformulation of these experiments.

Also, the CRPSO is used with a special encoding for the candidate particles, considering cardinality constraints limiting the maximum number of distinct cross-sectional areas to be used in an optimized solution. It seems clear that this can lead to economies of bulk purchasing, checking, welding, transportation and freeing the designer from the task of deciding how to group members and/or design variables.

Future work will consider, in the same optimization problems, static loads, self-weight loads and those arising from

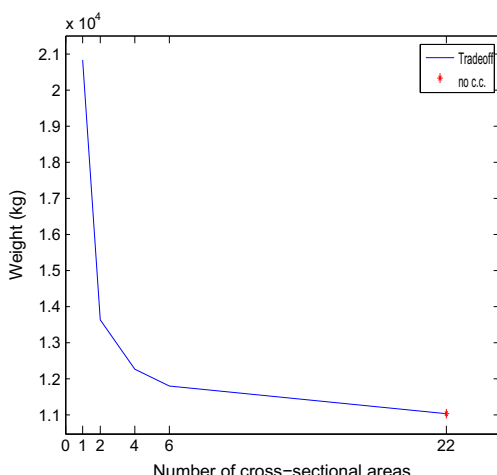


Fig. 71 The tradeoff between weight and number of sections for the 1410-bar truss dome

the environmental such as wind and earthquake dynamic actions. Topology optimization problems considering the best member grouping and the best material combination presenting nonlinear behavior discussed by Zhang et al. (2017) is an attractive point to be investigated in future works.

Also, other structures will be analyzed, such as plane and spatial frames. Multiobjective optimization is another point to be investigated where the designer will be able to define, for example, a range of natural frequencies to be satisfied. Meanwhile it is possible to find a set of non-dominated solutions and Pareto frontiers can be constructed offering a set of interesting solutions.

Recently, very important strategies are massively used in the literature to reduce the computational time of the optimization problems solved by using population-based meta-heuristics adopting surrogate models (Tenne and Goh 2010; Krempser et al. 2017).

Finally, as a future work, it is important to remark that it is possible to formulate and investigate a new optimization problem by using a more sophisticated fitness function that reflects the total costs associated with aspects related to fabrication, transportation, storing, checking, and so on.

Acknowledgments The authors wish to thank the referees that helped the quality of the paper, CNPq (305175/2013-0 e 305099/2014-0), FAPEMIG (TEC PPM 528/11, TEC PPM 388/14 and TEC APQ 00103-12) and CAPES for their support.

References

- Achziger W (1996) Truss topology optimization including bar properties different for tension and compression. *Structural Optimization* 12(1):63–74
- Achziger W (1997) Topology optimization of discrete structures. *Topology Optimization in Structural Mechanics*. Springer, pp 57–100
- Achziger W (1999) Local stability of trusses in the context of topology optimization part i: exact modelling. *Struct Optim* 17(4):235–246
- Achziger W (1999) Local stability of trusses in the context of topology optimization part ii: a numerical approach. *Struct Multidiscip Optim* 17(4):247–258
- Achziger W, Kočvara M (2007) On the maximization of the fundamental eigenvalue in topology optimization. *Struct Multidiscip Optim* 34(3):181–195
- Achziger W, Kočvara M (2007) Structural topology optimization with eigenvalues. *SIAM J Optim* 18(4):1129–1164
- Angelo JS, Bernardino H, Barbosa H (2015) Ant colony approaches for multiobjective structural optimization problems with a cardinality constraint. *Adv Eng Softw* 80:101–115
- Barbosa HJC, Lemonge ACC (2002) An adaptive penalty scheme in genetic algorithms for constrained optimization problems GECCO, vol 2, pp 287–294
- Barbosa HJC, Lemonge ACC (2005) A genetic algorithm encoding for a class of cardinality constraints. In: Proceedings of the 7th annual conference on genetic and evolutionary computation. ACM Press, pp 1193–1200
- Barbosa HJC, Lemonge ACC, Borges CCH (2008) A genetic algorithm encoding for cardinality constraints and automatic variable linking in structural optimization. *Eng Struct* 30:3708–3723
- Bathe KJ (2006) Finite element procedures. Prentice Hall, Pearson Education Inc
- Bellagamba L, Yang T (1981) Minimum-mass truss structures with constraints on fundamental natural frequency. *AIAA J* 19(11):1452–1458
- Biedermann JD (1997) Representing design knowledge with neural networks. *Comput-Aided Civil Infrastruct Eng* 12(4):277–285
- Biedermann JD, Grierson DE (1995) A generic model for building design. *Eng Comput* 11(3):173–184
- Biedermann JD, Grierson DE (1996) Training and using neural networks to represent heuristic design knowledge. *Adv Eng Softw* 27(1):117–128
- Carvalho ECR, Bernardino H, Hallak PH, Lemonge ACC (2015) An adaptive penalty scheme to solve constrained structural optimization problems by a CRPSO. *Optim Eng*. To appear
- Chun J, Song J, Paulino GH (2012) Topology optimization of structures under stochastic excitations. In: 2012 joint conference of the engineering mechanics institute and the 11th ASCE joint specialty conference on probabilistic mechanics and structural reliability
- Eberhart R, Kennedy J (1995) A new optimizer using particle swarm theory. In: Proceedings of the 6th international symposium on micro machine and human science, 1995. MHS'95. IEEE, pp 39–43
- Farshchin M, Camp CV, Maniat M (2016) Multi-class teaching-learning-based optimization for truss design with frequency constraints. *Eng Struct* 106:355–369
- Filipov ET, Chun J, Paulino GH, Song J (2016) Polygonal multiresolution topology optimization (polymtop) for structural dynamics. *Struct Multidiscip Optim* 53(4):673–694
- Galante M (1996) Genetic algorithms as an approach to optimize real-world trusses. *Int J Numer Methods Eng* 39(3):361–382
- Gomes HM (2011) Truss optimization with dynamic constraints using a particle swarm algorithm. *Expert Syst Appl* 38(1):957–968
- Grierson DE, Cameron GE (1987) Soda-structural optimization design and analysis. Waterloo Engineering Software, Ontario
- Herencia JE, Haftka RT (2010) Structural optimization with limited number of element properties. *Struct Multidiscip Optim* 41(5):817–820
- Herencia JE, Haftka RT, Balabanov V (2013) Structural optimization of composite structures with limited number of element properties. *Struct Multidiscip Optim* 47(2):233–245
- Kar R, Mandal D, Mondal S, Ghoshal SP (2012) Craziness based particle swarm optimization algorithm for fir band stop filter design. *Swarm and Evolutionary Computation*
- Kaveh A, Farhoudi N (2011) A unified approach to parameter selection in meta-heuristic algorithms for layout optimization. *J Construct Steel Res* 67(10):1453–1462
- Kaveh A, Farhoudi N (2013) A new optimization method: Dolphin echolocation. *Adv Eng Softw* 59:53–70
- Kaveh A, Ghazaan MI (2016) Optimal design of dome truss structures with dynamic frequency constraints. *Struct Multidiscip Optim* 53(3):605–621
- Kaveh A, Jafari L, Farhoudi N (2015) Truss optimization with natural frequency constraints using a dolphin echolocation algorithm. *Asian J Civil Eng* 16:29–46
- Kaveh A, Jafari L, Farhoudi N (2015) Truss optimization with natural frequency constraints using a dolphin echolocation algorithm. *Asian j Civil Eng (BHRC)* 16(1):29–46
- Kaveh A, Javadi S (2014) Shape and size optimization of trusses with multiple frequency constraints using harmony search and ray optimizer for enhancing the particle swarm optimization algorithm. *Acta Mechanica* 225(6):1595–1605

- Kaveh A, Zolghadr A (2011) Shape and size optimization of truss structures with frequency constraints using enhanced charged system search algorithm. *Asian J Civil Eng* 12(4):487–509
- Kaveh A, Zolghadr A (2012) Truss optimization with natural frequency constraints using a hybridized css-bbbc algorithm with trap recognition capability. *Comput Struct* 102:14–27
- Kaveh A, Zolghadr A (2014) Democratic PSO for truss layout and size optimization with frequency constraints. *Comput Struct* 130:10–21
- Konzelman CJ (1986) Dual methods and approximation concepts for structural optimization. Department of Mechanical Engineering U.O.T
- Krempser E, Bernardino HS, Barbosa H, Lemonge A, de Castro C (2017) Performance evaluation of local surrogate models in differential evolution based optimum design of truss structures. *Eng Comput* 34(2):499–547
- Kripka M, Medeiros GF, Lemonge ACC (2013) Structural optimization of reinforced concrete building grillages considering cardinality constraints. In: 10th world congress on structural and multidisciplinary optimization, pp 01–06
- Kripka M, Medeiros GF, Lemonge ACC (2015) Use of optimization for automatic grouping of beam cross-section dimensions in reinforced concrete building structures. *Eng Struct* 99:311–318
- Lemonge A, Barbosa H, Coutinho A, Borges C (2011) Multiple cardinality constraints and automatic member grouping in the optimal design of steel framed structures. *Eng Struct* 33:433–444
- Lemonge ACC, Barbosa HJC, Coutinho ALGA, Borges CCH (2011) Multiple cardinality constraints and automatic member grouping in the optimal design of steel framed structures. *Eng Struct* 33(2):433–444
- Lemonge ACC, Barbosa HJC, da Fonseca LG, Coutinho ALGA (2010) A genetic algorithm for topology optimization of dome structures. In: Proceedings of the 2nd international conference on engineering optimization EngOpt
- Lin J, Che W, Yu Y (1982) Structural optimization on geometrical configuration and element sizing with statical and dynamical constraints. *Comput Struct* 15(5):507–515
- Lingyun W, Mei Z, Guangming W, Guang M (2005) Truss optimization on shape and sizing with frequency constraints based on genetic algorithm. *Comput Mech* 35(5):361–368
- Liu X, Cheng G, Wang B, Lin S (2012) Optimum design of pile foundation by automatic grouping genetic algorithms. *ISRN Civil Engineering*
- Liu X, Cheng G, Yan J, Jiang L (2012) Singular optimum topology of skeletal structures with frequency constraints by AGGA. *Struct Multidiscip Optim* 45(3):451–466
- Miguel LFF, Miguel LFF (2012) Shape and size optimization of truss structures considering dynamic constraints through modern metaheuristic algorithms. *Expert Syst Appl* 39(10):9458–9467
- Nakamura T, Ohsaki M (1992) A natural generator of optimum topology of plane trusses for specified fundamental frequency. *Comput Methods Appl Mech Eng* 94(1):113–129
- Ohsaki M (2016) Optimization of finite dimensional structures. CRC Press
- Rajan S (1995) Sizing, shape, and topology design optimization of trusses using genetic algorithm. *J Struct Eng* 121(10):1480–1487
- Rajeev S, Krishnamoorthy C (1992) Discrete optimization of structures using genetic algorithms. *J Struct Eng* 118(5):1233–1250
- Rubio WM, Paulino GH, Silva ECN (2011) Tailoring vibration mode shapes using topology optimization and functionally graded material concepts. *Smart Mater Struct* 20(2):025,009
- Sedaghati R (2005) Benchmark case studies in structural design optimization using the force method. *Int J Solids Struct* 42(21):5848–5871
- Shea K, Cagan J, Fenves SJ (1997) A shape annealing approach to optimal truss design with dynamic grouping of members. *J Mech Des* 119(3):388–394
- Stolpe M (2016) Truss optimization with discrete design variables: a critical review. *Struct Multidiscip Optim* 53(2):349–374
- Tejani GG, Savsani VJ, Patel VK (2016) Adaptive symbiotic organisms search (SOS) algorithm for structural design optimization. *Journal of Computational Design and Engineering*
- Tejani GG, Savsani VJ, Patel VK (2016) Modified sub-population teaching-learning-based optimization for design of truss structures with natural frequency constraints. *Mechanics Based Design of Structures and Machines*
- Tenne Y, Goh CK (2010) Computational intelligence in expensive optimization problems, vol. 2 Springer Science and Business Media
- Vargas DEC, Lemonge ACC, Barbosa HJC, Bernardino H (2015) Um algoritmo baseado em evolução diferencial para problemas de otimização estrutural multiobjetivo com restrições. *Revista Internacional de Métodos Numéricos para Cálculo y Diseño en Ingeniería*. (in portuguese)
- Wang D, Zhang W, Jiang J (2004) Truss optimization on shape and sizing with frequency constraints. *AIAA J* 42(3):622–630
- Zhang X, Ramos AS, Paulino GH (2017) Material nonlinear topology optimization using the ground structure method with a discrete filtering scheme. *Struct Multidiscip Optim* 55(6):2045–2072